Endocrinology, 2025, **166**, bqaf126
https://doi.org/10.1210/endocr/bqaf126
Advance access publication 4 August 2025
Research Article

Pig Taste Cell-derived Organoids Synthesize Insulin

Hasitha U. Premathilake,[1] Caio H. Mazucanti,[1] Qin Yao,[1] Jennifer F. O'Connell,[1] Nandita Vegesna,[1] Dimitrios Tsitsipatis,[2] Cory Weller,[3] Kwan-Wood Gabriel Lam,[4] Julián Candia,[5] Jinshui Fan,[4] Supriyo De,[4] Payel Sen,[2] Josephine M. Egan,[1] and Máire E. Doyle[1]

[1]Laboratory of Clinical Investigation, National Institute on Aging, Intramural Research Program, National Institutes of Health, Baltimore, MD 21224, USA
[2]Laboratory of Genetics and Genomics, National Institute on Aging, Intramural Research Program, National Institutes of Health, Baltimore, MD 21224, USA
[3]Center for Alzheimer's and Related Dementias, National Institute on Aging, Intramural Research Program, National Institutes of Health, Bethesda, MD 21224, USA
[4]Computational Biology and Genomics Core, National Institute on Aging, Intramural Research Program, National Institutes of Health, Baltimore, MD 21224, USA
[5]Longitudinal Studies Section, Translation Gerontology Branch, National Institute on Aging, Intramural Research Program, National Institutes of Health, Baltimore, MD 21224, USA

Correspondence: Máire E. Doyle, PhD, National Institute on Aging, 251 Bayview Blvd, Ste 100, Baltimore, MD 21224, USA. Email: doyleme@nih.gov.

Abstract

Here we describe organoid cultures derived from pig foliate taste papillae in which the cellular heterogeneity of the lingual epithelium is preserved. Pig taste organoids were maintained long term (18 passages) and continued to express taste stem cell markers *(LGR4, LGR6,* and *SOX2*) and taste receptor cell (TRC) markers (cytokeratin 20, *ENTPD2, GNAT3,* and *OTOP1*). We show insulin is necessary for optimum proliferation and differentiation of taste organoids. Some TRCs in the organoids contained insulin and the insulin-critical transcription factors *MAFA* and *PAX4*. However, we did not see any evidence of the critical glucose-responsive *PDX-1* expression either in the native tissue or in the organoids. We optimized differentiation conditions for TRC expression and separately for increased insulin protein content (6.5-fold, $P < .01$ vs spontaneous differentiation). Insulin production in differentiated organoids was responsive to cAMP stimuli. These results provide a pig model of taste organoid culture that can be used to study taste stem cell dynamics and taste receptor cell differentiation. These findings suggest that taste organoids may serve as a novel renewable model system for studying extra-pancreatic, nonglucose-regulated insulin and its potential role as a trophic factor.

Key Words: taste organoids, taste stem cells, taste receptor cells, gustatory, insulin, dynamic 3D culture

Studies in taste progenitor cell homeostasis and preservation of taste buds with their cellular components received renewed interest during the COVID-19 pandemic (1-3). Despite the sense of taste being essential to determining the quality and contents of foods and the ease of access to taste buds and their progenitor cells for investigation, very little is known about the nature of taste progenitor cells and how they function in age and disease. Taste receptor cells (TRCs) that reside within taste buds of the tongue epithelium are responsible for sensing all 5 prototypic tastes—bitter, sweet, umami, sour, and salty. TRCs are highly complex sensory cells that are fully differentiated and do not undergo replication. Moreover, they exist in a mechanically stressful environment and must be replaced from progenitor cells located in the intragemmal regions of the lingual epithelium (4). TRCs continually sample the environment of the mouth, are vulnerable to infection as has again been emphasized by the COVID-19 virus, and deploy elements of the innate immune system as a first line of defense (5). Therefore, to gain a more in-depth molecular understanding of taste progenitor cells, taste bud differentiation, and immune response within taste buds, it would be useful to have an in vitro model that could conveniently be studied by researchers across these disciplines. Since their development (6), organoid cultures have allowed us to probe differentiation and renewal in many organ types in vitro. To date, taste organoids that contain taste stem cells, non-taste epithelium, taste progenitor cells, and mature TRCs have been cultured from genetically labelled LGR5- (7) and SOX2- (8) cells of mice. We and others have also shown that TRCs express several gut hormones, some of which have been demonstrated to modulate taste perception (2). Egan and coworkers have shown that GLP-1 is expressed on the subset of type II cells that express T1R3 and α-gustducin and GLP-1 receptor knockout mice show dramatically reduced taste responses to sweeteners in a behavioral assay (9); glucagon is restricted to type II cells that express T1R3, and mice lacking the chaperone protein 7B2 required for PC2 activation and the production of mature glucagon have

Received: 6 March 2025. **Editorial Decision:** 30 July 2025. **Corrected and Typeset:** 22 August 2025
Published by Oxford University Press on behalf of the Endocrine Society 2025.
This work is written by (a) US Government employee(s) and is in the public domain in the US. See the journal About page for additional terms.

Downloaded from https://academic.oup.com/endo/article/166/9/bqaf126/8221664 by Odense Universitetsbibliotek user on 21 April 2026

reduced sensitivity to sucrose (10). Intriguingly, we found (11) that mammalian TRCs make biologically active insulin and C-peptide, yet another source of extra-pancreatic insulin in addition to the choroid plexus (12). Given the constant requirement for regeneration of the TRC precursors, local expression of insulin may play a role in autocrine or paracrine signaling mechanisms that regulate taste cell turnover. Therefore, we required a more relevant large animal model (13) that is more clinically relevant to decipher how insulin is involved in TRC development and renewal. We also wanted a model in which we could examine the function of insulin in relation to stem cell proliferation and differentiation.

The pig is a good model for taste organoid studies, and nutrient-sensing mechanisms are largely conserved between humans and pigs (14). Here we present a detailed characterization of pig taste organoid cultures maintained long term in culture for more than 18 passages over 3 years. We optimized an LGR4/6 promoting media, which we applied in dynamic suspension culture of organoids to enhance expression of TRC markers. To demonstrate how pig taste organoids can be used by both taste researchers and as a model to study extra-pancreatic insulin production, we developed 2 separate protocols to (1) enhance their differentiation into mature taste organoids containing cells expressing TRC markers (2) induce quiescence through inhibition of the MAPK, Notch, and Wnt/β catenin pathways to increase insulin protein levels. This work provides a new model to study TRC renewal and development, addresses the question of the function of insulin in taste stem cell proliferation and differentiation, and describes a regulatory mechanism for the production of insulin in TRCs.

Materials and Methods

Tissue Harvesting and Establishment of Primary Porcine Foliate Organoid Cultures

The foliate papillae (FP) were dissected from postmortem pig tongue, further dissected into ~1 mm^2 pieces, and digested using collagenase P containing digestion media (Fig. 1A). The tissue digestion was washed and filtered through a 100 µm filter (to include single cells and small tissue/cell clumps) and plated using base membrane extract (BME), thus giving rise to small reticulate taste organoids within 2 days in the LGR6 promoting media (LPM). Organoids in passage 0 (P.0) originated from both single cells and small cell/tissue clumps. Established organoids were passaged approximately every 14 to 15 days, and at the time of writing the maximum number of passages reached was 18. Fresh pig tongues were obtained from Wagner Meats (Mount Airy, MD) a US Department of Agriculture-monitored abattoir. The posterior of the tongue where the FP are located was sprayed with 80% ethanol. Foliate papillae were removed using a sterile disposable scalpel and rinsed in 50 mL of fresh PBS/Primocin (50 ng/mL, InvivoGen, San Diego, CA), which was also used for transport to the lab at 4 °C. Tissue pieces were then dissected using disposable scalpels to obtain 1 mm^2 size tissue pieces. Tissue pieces were then transferred into a 50 mL tube containing 20 mL of digestion medium made with LGR6 base media (LBM), 1 mg/mL collagenase P (Roche, Cat# 11213873001), DNAse (Sigma-Aldrich, Cat# D4527-200KU), 10 µM Y27632 (Biogems, Cat# 129823-10MG), and 20 × 3 mm diameter silicon nitride beads (MSE Supplies, Cat# BAO803), which was then placed in an orbital shaker (37 °C, 300 rpm) for 1 hour. Tubes were next placed on ice with 25 mL of wash media (DMEM/F12, 100 µg/mL primocin, 2% B27, and 10 µM Y27632) and centrifuged at 400 g for 10 minutes at 4 °C. The supernatant was discarded, 25 mL of fresh wash media was added, and the samples were washed a further 3 times. After the final wash, each individual reaction was filtered through a 100 µm filter and centrifuged as before. The pelleted cells were mixed with 3 mL of Cultrex™ RGF BME type 2 (R&D Systems, Cat# 3533-005-02) and plated in ~10 × 10 µL sized domes on each well of 6-well plate using a 200 µL pipette while frequently pipetting up and down to homogenize the solution. The plates were placed upside down for 20 minutes at 37 °C in a CO_2 incubator and then fed with LPM supplemented with ROCK inhibitor Y-2763. LPM was made by adding the following peptides and small molecules to LBM: epidermal growth factor (50 ng/mL), fibroblast growth factor (FGF) 10 (100 ng/mL), FGF2 (10 ng/mL), R-spondin-2 (RSO2; 500 ng/mL), Noggin (100 ng/mL), human sonic hedgehog (SHH; 100 ng/mL), Y-27632 (10 µM) from Peprotech, human wingless-related integration site 3A (Wnt3a; 100 ng/mL) from R&D Systems, insulin (10 nM) from Gibco, A-83-01 (0.5 µM), SB202190 (10 µM), CHIR99021 (2.5 µM), prostaglandin E2 (PGE2; 20 nM) from BioGems, forskolin (1 µM) from Tocris, and nicotinamide (10 mM) from Sigma-Aldrich. LBM was made by adding the following to DMEM/F12 GlutaMAX from Gibco: hepes (10 mM) and B27 insulin free (2%) from Gibco, N21 Max insulin free (2%) from R&D Systems, and Primocin (10 µg/mL) from InvivoGen. All peptides were dissolved in PBS containing 0.01 mg/mL human serum albumin (Sigma-Aldrich, Cat# A9511) prior to addition to the media. Organoid-like structures were visible emerging from the tissue pieces after 3 days in culture.

Long-term Culture of Taste Organoids

The plated organoid cultures were fed fresh LPM every 48 to 72 hours. Passaging was done every 14 days using TrypLE™ Express Enzyme (Thermo Fisher Scientific, Cat# 12605010). Domes containing ~day 14 organoids were washed twice using 2 mL PBS (Thermo Fisher Scientific, Cat# 10010023) for each well of a 6-well plate (or 1 mL in a 12-well plate) prior to adding 1 mL TrypLE Express Enzyme to each well. The domes were dislodged using a cell lifter and transferred along with the dissociation media into 15 mL conical tube (multiple wells of the same cell line could be combined) and incubated at 37 °C in a bead bath for 10 minutes, triturating every 5 minutes using a 1000 µL pipette fitted with maximum recovery tips. The dissociation enzyme was then diluted with wash media (LBM supplemented with Y-27632) and centrifuged at 400 g at 4 °C for 4 minutes. The pelleted cells were washed once and filtered through a 37-micron filter to obtain a single-cell solution. Total cell counts were measured using the Moxi Z™ cell counter (Oroflo, El Cajon, CA) and plated at a density of 5×10^4 cells/50 µL of Cultrex BME Type 2. Cultures were tested for the presence of mycoplasma using the MycoStrip mycoplasma kit (InvivoGen, San Diego, CA) according to the manufacturer's instructions and were found to be negative.

Cryopreservation and Recovery of Porcine Foliate Taste Organoid Cultures

Single cells obtained during passaging via dissociation and filtering (see previous discussion) were spun down and

Downloaded from https://academic.oup.com/endo/article/166/9/bqaf126/8221664 by Odense Universitetsbibliotek user on 21 April 2026

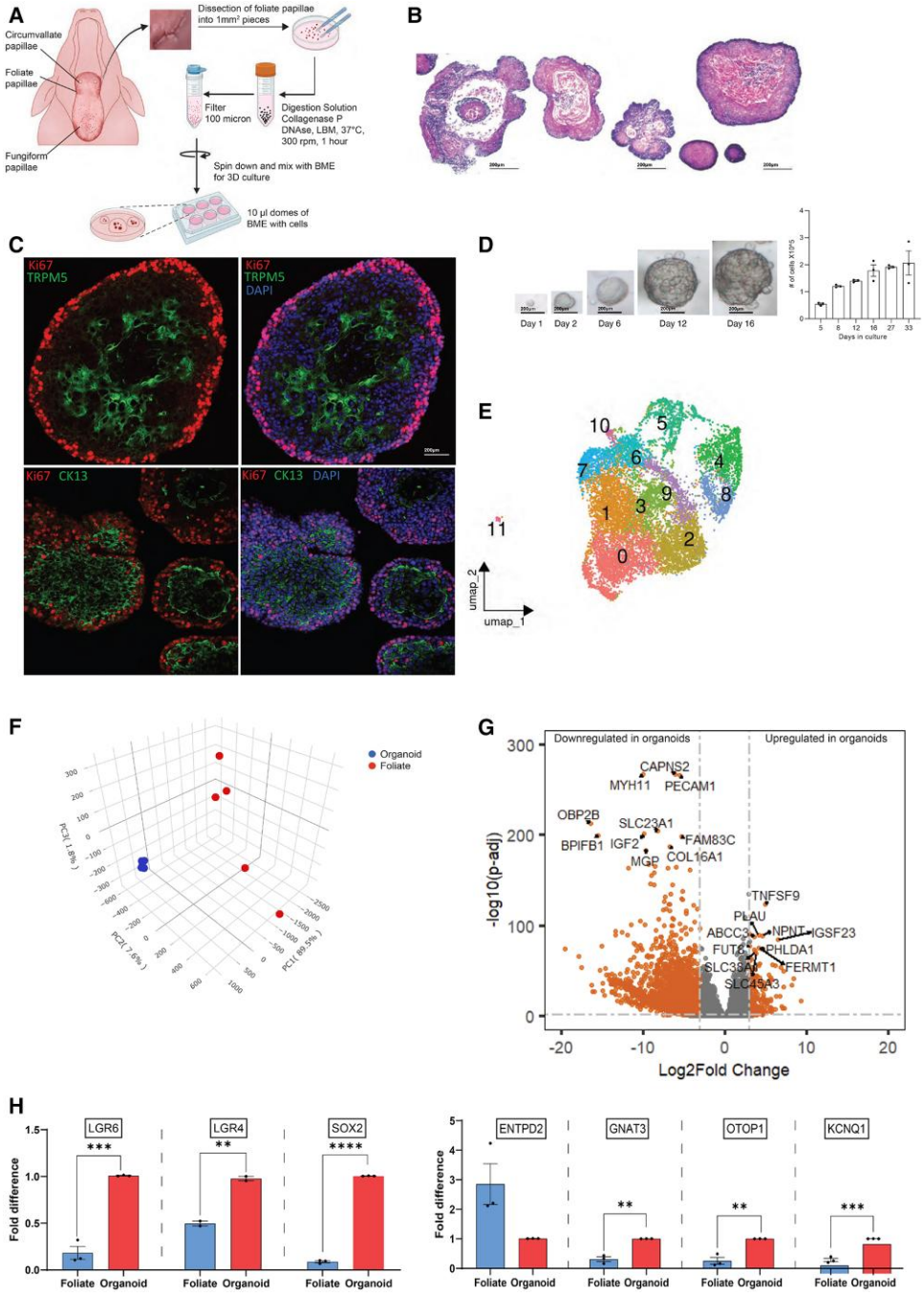


Figure 1. Growth dynamics, spontaneous differentiation, and transcriptomics of LGR4$^+$/LGR6$^+$ expressing porcine foliate organoids. (A) The foliate papillae were dissected from the pig tongue, cut into 1 mm^2 pieces, and digested in collagenase P, DNAse, in Lgr4/6 base medium at 37 °C, 300 rpm for 1 hour under sterile conditions. The resulting digest was filtered through a 100-micron filter, mixed with Cultrex, and plated as 10 µL domes in a 6-well plate. The culture was fed with LPM every 2 to 3 days. The initial feed following plating was supplemented with Y27632 ROCK inhibitor (10 nM). (B) Typical histology of early passage organoids, hematoxylin and eosin staining, depicting morphologies of (left to right) organoid within organoid, budding, and reticulate. (C) Immunohistochemistry of mature taste organoids depicting a proliferating (Ki67$^+$) outer cell layer and a differentiated center positive for TRPM5 (top) and CK13 (bottom), thus indicating the presence of mature type II TRCs and epithelial cells, respectively. (D) Growth and expansion of taste organoid cultures from single cells to mature taste organoids over a 16-day period. The number of cells in culture increased exponentially until day ~14 to 16 and plateaued thereafter. Data show 1 of 2 representative experiments, n = 3. (E) UMAP representation of genes found in single-cell RNA sequencing analysis of pig taste organoids harvested on day 14 (n = 2), colored by cluster of cell type. See Table 2 for cell cluster assignment (n = 2; UMAP shows the combination of the 2 conditions). (F) Three-dimensional principal component analysis plot based on poly(A) enriched RNA sequencing analysis of taste organoid samples (n = 5) vs its complementary native taste tissue (n = 5). The organoids and their native tissue counterpart form 2 separate clusters indicating the heterogenicity in their gene expression profiles. (G) Volcano plot depicting the DEGs in taste organoids compared to native tissue (n = 5). A total of 2396 genes were upregulated while 6536 were downregulated, based on a threshold criterion of |log 2 foldchange| > 1 and false discovery rate < 0.05. The top 10 most upregulated/downregulated DEGs are labeled. (H) Quantitative RT-PCR analysis of gene expression in the taste organoids vs foliate native tissue (n = 3 separate pigs and their corresponding organoids) indicating the expression and significant upregulation of taste stem cell, taste progenitor cell, and TRC markers (except *ENTPD2*) in organoids grown in LPM. ***$P < .001$, **$P < .01$, *$P < .05$. Data are presented as mean ± SEM. *P*-values were calculated using ANOVA. Scale bar, 200 µm.

Abbreviations: DEG, differentially expressed gene; LPM, Lgr4/6 promoting medium; TRC, taste receptor cell.

Downloaded from https://academic.oup.com/endo/article/166/9/bqaf126/8221664 by Odense Universitetsbibliotek user on 21 April 2026

resuspended in ~1 mL CryoStor® CS10 (STEMCELL, Cat# 100-1061), transferred to a 2 mL cryotube, and immediately stored in a Cryo 1 °C Freezing Container (NALGENE, Cat# 5100-0001) at −80 °C overnight and subsequently stored in N_2(L) until recovery. The cryopreserved cells were recovered by rapidly thawing the cryotube in a 37 °C bead bath. Cells in CryoStor were added dropwise into 9 mL of LPM in room temperature, spun down (as previously) and re-plated on a 6-well plate using 700 µL of BME, fed, and expanded as previously mentioned.

Time Series Imaging of Organoid Expansion

Taste organoid growth from days 5 to 15 was captured using the Celldiscoverer 7 (Zeiss). Taste organoids were plated as described previously in a 24-well plate at standard density and maintained in a humidified incubator at 37 °C with 5% CO_2 in the instrument. Brightfield images were taken using a 5X objective every 2 hours for over the 10 days using automatic exposure. Acquired images and video were processed using Zen 3.1 Blue (Zeiss).

Dynamic Culture of Taste Organoids in ClinoStar® and Their Harvesting

The dynamic porcine taste organoid cultures were established using the ClinoStar® clinostat CO_2 incubator system (Celvivo, Odense, Denmark). The ClinoReactors® are culture chambers (10 mL) with hydro beads and a semipermeable membrane that ensures a constant volume of culture media and CO_2 equilibrium. The hydro beads were hydrated overnight using 25 mL sterile water, and the ClinoReactors were equilibrated using 5 mL of LPM (in the culture chamber) by spinning them inside the ClinoStar for at least 4 hours before routine use.

Mature porcine taste organoids grown in LPM (day 14 and beyond) were dissociated into single cells as described previously, and 1.8×10^6 cells were spun down (at 4 °C, 400 g for 6 minutes) and resuspended in LPM (100 µL). The cell suspension was mixed well with 200 µL of xeno-free VitroGel® Hydrogel Matrix (The Well Bioscience, Monmouth Junction, NJ, Cat# VHM01) to give a final cell solution of 6000 cells/µL and kept on ice until needed. The culture chamber of the ClinoReator was filled with 5 mL of LPM and was positioned in the petri dish mode and the front lid opened. Ten µL droplets of VitroGel cell suspension were added into the ClinoReactor by gently touching the surface of the media. The culture chamber was resealed by closing the front lid, and the remaining 5 mL LPM was added to fill up the ClinoReactor. The ClinoReactors were then placed on the rotor of the ClinoStar for incubation at 37 °C and 5% CO_2. The rotation was adjusted accordingly to keep organoids in the middle of the spinning culture chamber, thus preventing them from hitting a peripheral membrane. The dynamic cultures were fed every 2 days by replacing 5 mL of spent media with 5 mL of fresh LPM. The ClinoReactor was changed every 10 to 12 days, and all media changes were done via the top access port (with the stopper) using blunt-needled syringes (10 mL) as recommended by the manufacturer.

The harvesting of dynamic culture organoids was done using the VitroGel Organoid Recovery Solution (The Well Bioscience Inc., Cat# MS04-100). The ClinoReactor containing the organoid culture was removed from ClinoStar incubator and placed upright for the organoids to settle on the bottom, and 5 mL of media was removed using the top access port. Subsequently, using the ClinoReactor in petri dish mode, the remaining media and organoids were moved to a 15 mL conical tube (accessing the culture chamber via the front lid) and spun down at 400 g, 4 °C for 4 to 6 minutes to pellet the organoids. Culture media was aspirated out, and the organoids were washed 2 times with 5 mL of ice-cold PBS (Thermo Fisher Scientific, Cat# 10010023). Five mL of prewarmed (37 °C) organoid recovery solution was added and incubated at 37 °C for 3 to 5 minutes, followed by rocking of the tubes 20 times. The full dissociation of the VitroGel ECM took at least 2 iterations of this incubation process. Subsequently, the tube was spun down at 400 g, 4 °C for 6 minutes to collect the organoid pellet and subject to downstream processing.

Optimization of Culture Conditions to Improve Differentiation

Organoid cultures were established and grown from day 0 to day 10 in LPM as described previously. On day 10 taste organoids, they were then fed with C5 media containing epidermal growth factor (50 ng/mL), FGF2 (100 ng/mL), FGF10 (100 ng/mL), RSO2 (100 ng/mL), Noggin (100 ng/mL), insulin (10 nM), IGF1 (100 ng/mL), IGF2 (100 ng/mL), IL22 (2 ng/mL), PGE2 (20 nM), forskolin (1 µM), DAPT (50 µM), and exendin-4 (5 nM). For all differentiation experiments conducted, the organoids in C5 media were harvested on day 16/17.

In order to improve the total insulin synthesis, the day 10 taste organoids grown in LPM were fed with quiescence condition (CQ) media containing FGF2 (100 ng/mL), FGF10 (100 ng/mL), RSO2 (100 ng/mL), Noggin (100 ng/mL), insulin (10 nM), IGF1 (100 ng/mL), IGF2 (100 ng/mL), IL-22 (2 ng/mL), PGE2 (20 nM), forskolin (1 µM), DAPT (50 µM), exendin-4 (5 nM), SCH772984 (10 nM), mirdametinib (5 nM), afatinib (10 nM), AZD-8055 (0.1 nM), gefitinib (5 nM), IWP-2 (1.5nM), and AS1842856 (1 nM). Similar to C5 organoids, all CQ organoids used in subsequent experiments were harvested on day 16 or 17, depending on the experiment.

Organoid Harvesting (Static Culture), RNA Isolation, cDNA Synthesis, and Quantitative RT-PCR Analysis

Organoid harvesting from 6-well/12-well plates was done using the Cultrex Organoid Harvesting Solution (Cat# 3700-100-01). Briefly, working on ice, the cell culture media was gently aspirated, and each well was washed with PBS (2 mL/1 mL). One ml of the organoid harvesting solution was added to each well; then the domes were gently dislodged using a cell scraper/lifter and incubated for 1 hour at 4 °C on a rocking shaker (Reliable Scientific Inc.) at a speed of 50, for BME digestion. Postincubation, the organoids were spun down and washed 3 times, again with 1 mL PBS. Each spin down was done at 400 g for 4 minutes at 4 °C. The pelleted organoids from each well were next lysed in 600 µL of RLT Plus lysis buffer (Qiagen) with 6 µL of ß-mercaptoethanol (Sigma Life Science, Cat# 63689-100ML-F) and homogenized using ~200 µL of 1.0 mm Zirconia (BioSpec, Cat# 11079110ZX) beads with a single 30-second, 6000 rpm cycle on a Precellys24 homogenizer (Bertin Corp.). The homogenized solution was spun down for 20 minutes at 8000 rpm prior to RNA isolation using RNEasy Plus Mini Kit (Qiagen, Cat# 74134/74136) according to the manufacturer's

Downloaded from https://academic.oup.com/endo/article/166/9/bqaf126/8221664 by Odense Universitetsbibliotek user on 21 April 2026

protocol. Porcine FP were homogenized in the extraction buffer provided in the Arcturus™ PicoPure™ RNA Isolation Kit (Applied Biosystems, Cat# 12204-01) using the same bead-based method described earlier. RNA extraction followed the recommended Arcturus PicoPure RNA Isolation Kit protocol without performing the DNAse step since TaqMan probes are at the junctions of gene exons. Single-strand cDNA was synthesized from total RNA using qScript™ Ultra SuperMix (QuantaBio, Cat# 95217-100) according to the recommended protocol. Quantitative RT-PCR (qRT-PCR) analyses were done using commercial TaqMan Fast Advanced Master Mix™ (Cat# 4444557), and the relevant TaqMan probes from Thermo Fisher Scientific [Supplementary Table S1 (15)] on an Applied BiosystemsViia7 384well qRT-PCR machine according to the recommended protocol. Porcine β-2-microglobulin was used as the housekeeping gene in all qRT-PCR analyses. All data are presented as mean ± SEM, and statistical differences were calculated using ANOVA in the software GraphPad Prism (Boston, MA).

Chinese Hamster Ovary-Insulin Receptor Cell Treatment and Immunoblotting

Chinese hamster ovary expressing the insulin receptor (CHO-IR) cells were cultured as described previously (16). Prior to treatment, the cells were washed 3 times with PBS and serum starved for 5 hours before being treated with insulin or insulin extracts for 5 minutes (1 and 10 nM). The cells were then washed in ice-cold PBS before being lysed in ice-cold RIPA buffer with protease inhibitors, sonicated (Qsonica, Newtown, CT), and centrifuged at 13 000 rpm for 10 minutes at 4 °C, and the supernatant was collected. Protein lysates were resolved by SDS-PAGE (4-12%) and then electroblotted onto polyvinylidene difluoride membranes. The membranes were probed overnight at 4 °C using the primary antibodies indicated in Table 1, followed by secondary antibodies conjugated to horseradish peroxidase (HRP) for 1 hour at room temperature. Immunoblots were developed with Super Signal West Femto HRP substrate (Thermo Fisher Scientific), exposed to HyBlot CL autoradiography film (Thomas Scientific, Swedesboro, NJ), and imaged using an SRX-101 film processor (Konica Minolta Medical Imaging, Wayne, NJ).

Porcine Taste Organoid mRNA Sequencing

Total RNA isolated from porcine foliate taste organoids (as mentioned previously) were sent out Novogene Inc. (Sacramento, CA) for mRNA sequencing (mRNA-Seq) library preparation and next-generation sequencing. mRNA was isolated from total RNA using poly-T oligo-attached magnetic beads. After fragmentation, first-strand cDNA was synthesized with random hexamer primers, followed by second-strand cDNA synthesis using dUTP to create a directional library. The library was prepared through a series of steps, including end repair, A-tailing, adapter ligation, size selection, USER enzyme digestion, amplification, and purification. It was then quantified using a Qubit fluorometer and real-time quantitative PCR, and the size distribution was verified with a bioanalyzer. The quantified libraries were pooled and sequenced on Illumina platforms, based on the effective library concentration and required data output. Index-coded samples were clustered following the manufacturer's instructions, and after cluster generation, sequencing was carried out on an Illumina platform to produce paired-end reads at a minimum

Table 1. Details of the antibodies

Antibody	Host species	Company	Catalog #	Purpose	RRID	Dilution
Anti-p-IRβ	Rabbit	Santa Cruz	sc-25103	Immunoblotting	RRID:AB_669389	1:500
Anti-IRβ	Rabbit	Santa Cruz	sc-711	Immunoblotting	RRID:AB_631835	1:1000
Anti-phospho-AKT (Ser473)	Rabbit	Cell Signaling	4060	Immunoblotting	RRID:AB_2315049	1:1000
Anti-phospho-IRS 1/2	Rabbit	Santa Cruz	sc-17195	Immunoblotting	RRID:AB_2127885	1:500
Anti-rabbit HRP	Donkey	Amersham	NA934	Immunoblotting	RRID:AB_772206	1:1000
Insulin	GP	Dako	IR002	Immunostaining	RRID:AB_2800361	1:50
Serotonin	Rabbit	Immunostar	20080	Immunostaining	RRID:AB_572263	1:1000
Ki67 antigen	Mouse	Agilent	M724001	Immunostaining	RRID:AB_2631211	1:100
CK13	GP	Acris	BP5076	Immunostaining	RRID:AB_979608	1:100
TRPM5	Rabbit	Sigma	HPA042115-100UL	Immunostaining	RRID:AB_2677854	1:100
CK20	Rabbit	Thermo Fisher Scientific	MA531979	Immunostaining	RRID:AB_2809273	1:100
CK14	Mouse	Abcam	ab9220	Immunostaining	RRID:AB_307087	1:100
Goat anti-rabbit IgG (heavy chain) superclonal secondary antibody, Alexa Fluor 488	Goat	Thermo Fisher Scientific	A27034	Immunostaining	RRID:AB_2536097	1:1000
Alexa Fluor 488 goat anti-guinea pig IgG (H + L) antibody, highly cross-adsorbed	Goat	Thermo Fisher Scientific	A11073	Immunostaining	RRID:AB_2534117	1:1000
Goat anti-rabbit IgG (H + L) highly cross-adsorbed antibody, Alexa Fluor 568 Conjugated	Goat	Thermo Fisher Scientific	A11036		RRID:AB_10563566	1:1000
goat anti-mouse IgG (H + L) highly cross-adsorbed antibody, Alexa Fluor 568 Conjugated	Goat	Thermo Fisher Scientific	A11031		RRID:AB_144696	1:1000

Downloaded from https://academic.oup.com/endo/article/166/9/bqaf126/8221664 by Odense Universitetsbibliotek user on 21 April 2026

sequencing depth of 20 million reads per sample. The raw data in FASTQ format were subjected to adapter sequence, poly-N sequence, and low-quality base removal using in-house perl scripts to obtain clean sequences that can be directly subjected to sequence alignment. All subsequent bioinformatic analyses were conducted using these clean, high-quality sequencing data. Raw data were deposited in the GEO database GSE252240.

Bioinformatic Analysis of Poly(A) Enriched RNA-Seq Data

Preprocessed (post-adapter and low-quality sequence removal) paired-end raw fastq sequences received from Novogene Inc. (Sacramento, CA) were analyzed using FastQC 0.11.9 for quality assurance and aligned against *Sus scrofa* 11.1 genome using the STAR aligner 2.7.10b in "GeneCounts" mode. Alignment quality for each sample was checked using MultiQC 1.14. Post-quality assurance, the resulting BAM files from STAR aligner were run through featureCounts in "countReadPairs" mode to obtain gene-wise transcript counts for each sample. A gene-wise count matrix was compiled for samples pertaining to each analysis (eg, organoids vs foliate, etc.) and subjected to subsequent differential gene expression analysis using DESeq2 available in Bioconductor version 3.17. The resulting normalized counts file and the differentially expressed genes (DEGs) file were used as the underlying data to generate all subsequent data visualizations such as principal component analysis (PCA), volcano plots, etc. R packages rgl 1.2.1 and EnhancedVolcano 1.18.0 were used to generate PCA plots and volcano plots, respectively. A threshold criterion of more than 20 normalized counts (median ratio normalization) in at least 1 replicate was used to determine the expression of a particular gene in organoid/foliate samples. This data was then used to identify genes unique/common to pig foliate tissue and foliate taste organoids using the "setdiff" function in R. Pathway enrichment analysis to derive canonical pathways was conducted using Ingenuity Pathway Analysis (IPA) by Qiagen and plotted using seaborn 0.12.2 and matplotlib 3.7.2 python packages. Gene set enrichment analysis (GSEA) was performed using the R package fgsea and the reference gene sets Reactome, KEGG, and WikiPathways available in the Molecular Signatures Database (17-20). The GSEA algorithm requires genes of interest to be preranked (postdifferential gene expression analysis); hence the metric "−log10 (*P*-value) * sign of fold change" that takes into account both the statistical significance in differential gene expression and directionality of the fold change was used for this purpose. R script developed in house (that implements a Monte Carlo algorithm over 1000 iterations) was used to add robustness to the inherently stochastic enrichment estimates and statistical significance generated by GSEA and hence uses the total statistical ensemble to choose significant enriched pathways that appear in more than 80% of the iterations (21).

Immunofluorescence Staining

Circumvallate papilla (CVP) tissue, FP, and harvested porcine taste organoids were cryosectioned (10 µm thick) using a Leica CM 1950 cryostat, mounted onto ColorFrost Plus Micro slides (Fisher Scientific) and then stored at −80 °C. Immunostaining was performed as described previously (11). To permeabilize the cells in the tissue, slides were placed in Tris-buffered saline (TBS; pH, 7.4; Quality Biologicals, Gaithersburg, MD) with 0.2% Triton-X 100 (Millipore Sigma) for 5 minutes at room temperature. They were then washed 3 times (2 minutes) in TBS. Antigen retrieval was performed by placing the slides in 10 mM of sodium citrate buffer (pH, 6.0; Vector Laboratories, Burlingame, CA) at 95 °C for 30 minutes. The slides were left to cool at room temperature in the citrate buffer for a further 30 minutes and were then rinsed in water and then TBS as before. Sections were incubated with normal goat serum block consisting of 2% goat serum, 1% OmniPur BSA Fraction V (Millipore Sigma), 0.1% gelatin (Millipore Sigma), 0.1% Triton X-100 (Millipore Sigma), 0.05% Tween 20 (Millipore Sigma), and 0.05% sodium azide (Millipore Sigma) in TBS for 1 hour at room temperature. Sections were then incubated with primary antibodies (Table 1) diluted in the same normal goat serum block at 4 °C overnight. Tissue sections were rinsed with TBS with 5% Tween and incubated for 1 hour with fluorescently labeled secondary antibodies (Table 1) at 1:1000 dilution, then washed with TBS with 5% Tween. After nuclear staining (4′,6-diamidino-2-phenylindole dihydrochloride, Sigma-Aldrich), sections were mounted with Fluoromount G (Southern Biotechnology, Birmingham, AL). Appropriate no-primary-antibody controls were prepared with each individual batch of slides. Confocal fluorescence images were captured using Zen Black Version 14 software on a Zeiss LSM-880 (Oberlochen, Germany) confocal microscope; brightness and contrast were adjusted globally. All figures were compiled in Adobe Illustrator 2021 (San Jose, CA).

Acid-ethanol Extraction of Insulin From Porcine CVP and Porcine Taste Organoids

Porcine foliate taste organoids grown in LPM and CQ media (passages 15-18), were harvested as described earlier and incubated in a sonicator bath/ultrasound cleaner (VWR, Symphony™) at 4 °C in 500 µL of acid-ethanol (0.18 M of HCl in 70:30 v/v ethanol:HCl) solution (11) overnight until the cell pellet was sufficiently lysed. The resulting supernatant (acid-ethanol) was neutralized using sodium hydroxide (an equimolar equivalent) and lyophilized using a benchtop freeze dryer (Labconco, FreeZone2.5). The concentration of the lyophilized insulin from LPM/CQ organoids was measured using the Mercodia Porcine Insulin (Cat# 10-1200-01, RRID:AB_2811079) ELISA kit. For insulin extraction from porcine CVP, the posterior of a fresh pig tongue (obtained from Wagner Meats, Mount Airy, MD) where CVP are located was sprayed with 80% and CVPs were removed using a sterile disposable scalpel and rinsed in 50 mL of fresh PBS/Primocin (50 ng/mL). The freshly dissected CVP was immediately subjected to acid-ethanol extraction of insulin as described previously (11). The insulin extracted from porcine CVP was used for CHO-IR cell treatment as described later. For experiments in which organoids were treated with forskolin, serotonin, or denatonium, the organoids were first removed from the BME using the Cultrex Organoid Harvesting Solution and were washed twice with DMEM/F12 without supplementation and then cultured overnight in DMEM/F12 with the reagents and then processed for insulin content measurement as described.

CHO-IR Cell Treatment and Immunoblotting

CHO-IR cells were cultured as described previously (16). Prior to treatment, the cells were washed 3 times with PBS and serum starved for 5 hours before being treated with

Downloaded from https://academic.oup.com/endo/article/166/9/bqaf126/8221664 by Odense Universitetsbibliotek user on 21 April 2026

insulin or insulin extracts for 5 minutes (1 and 10 nM). The cells were then washed in ice-cold PBS before being lysed in ice-cold RIPA buffer with protease inhibitors, sonicated (Qsonica, Newtown, CT), and centrifuged at 13 000 rpm for 10 minutes at 4 °C; then the supernatant was collected. Protein lysates were resolved by SDS-PAGE (4-12%) and then electroblotted onto polyvinylidene difluoride membranes. The membranes were probed overnight at 4 °C using the primary antibodies indicated in Table 1, followed by secondary antibodies conjugated to HRP for 1 hour at room temperature. Immunoblots were developed with Super Signal West Femto HRP substrate (Thermo Fisher Scientific) and exposed to HyBlot CL autoradiography film (Thomas Scientific, Swedesboro, NJ) and were imaged using an SRX-101 film processor (Konica Minolta Medical Imaging, Wayne, NJ).

Single Cell RNA-Seq of Pig Taste Organoids

Porcine foliate taste organoids grown in LPM were harvested on day 12 using the Cultrex Organoid Harvesting Solution (Cat 3700-100-01) for BME digestion and removal of BME fragments. The harvested organoids were then dissociated into single cells using TrypLE™ Express Enzyme (Thermo Fisher Scientific, Cat# 12605010) and filtered through a 37 µm sieve (following the protocol used to obtain single cells during organoid passaging mentioned earlier) to obtain single cells. The cell pellet was resuspended in PBS (Thermo Fisher Scientific, Cat# 10010023), and viability was assessed on the Countess II fluorescence automated cell counter (Thermo Fisher Scientific) and was greater than 80% so samples were immediately subjected to single-cell library construction using 10× Genomics Chromium Single Cell 3′ Reagent Kits v3.1 (10× Genomics, Cat# PN-1000269) with Chip G (10× Genomics, Cat# PN-1000127) following the manufacturer's protocol. Approximately 5000 to 10 000 individual cells were used to generate gel beads-in-emulsions. Post-gel beads-in-emulsions cleanup and cDNA synthesis were performed, and the quality was checked using the Agilent Bioanalyzer with the High-Sensitivity DNA kit (Agilent, Cat# 5067-4626). Library construction was done using the synthesized cDNAs, and the final libraries were evaluated using the 4200 TapeStation system with the DNA and High Sensitivity DNA 1000 ScreenTape. Sequencing was carried out on an Illumina NovaSeq 6000 sequencer. The number of cells from each organoid sample (n = 2) that were successfully sequenced and could be subjected to downstream statistical analysis and data visualization was 5129 and 6709. The resulting single-cell RNA-Seq data were subsequently deposited in GEO submission GSE252240 (22).

Bioinformatic Analysis of Single-cell RNA-Seq Data

Single-cell RNA-Seq (scRNA-Seq) samples were demultiplexed and mapped to the *Sus Scrofa* 11.1 reference genome using the Cell Ranger software version 8.0.1 (10× Genomics). "cellranger mkgtf" and "cellranger mkref" were used to build the reference *Sus scrofa* genome for Cell Ranger using Ensembl genome assemblies and GTF files pertaining to *Sus scrofa 11.1* genome assembly. The filtered feature matrices produced by "cellranger count" were used for downstream statistical analysis and data visualization using Seurat version 5.0.1 (23). Quality control filtering was applied to each sample to exclude empty droplets, low-quality cells, and potential doublets from downstream analysis by keeping the cells containing less than 1.5% mitochondrial genes and with unique feature count >200 and <7000. The 2 samples were combined using the Seurat "merge()" function and normalized using the "scTransform()" method (24) (vst.flavor = "v2"). Only the top 5000 variable genes were selected using the "FindVariableFeatures()" function for downstream analysis. IntegrateLayers(), FindNeighbors() method (dims = 1:12), FindClusters() method (resolution = 0.5), FindMarkers(), FindAllMarkers() were executed sequentially to integrate the cellular data in the 2 samples, cluster cells, and marker gene detection for each cluster using differential gene expression analysis. RunPCA(), RunUMAP(), and DoHeatmap () functions were used for dimensionality reduction data and data visualization, respectively. Assignment of clusters was based on prior knowledge of the cell types found in the oral lingual epithelium (2) and using the online gene set enrichment analysis tool Enrichr (25).

Statistical Data Analysis

All data are depicted as mean ± SEM unless otherwise specified. Statistical analysis was performed using GraphPad Prism v8.0 (GraphPad Software, San Diego, CA). Unpaired 2-tailed Student's *t*-test or 1-way ANOVA followed by Tukey's post hoc test was used to assess statistical significance as appropriate. *P*-values of less than .05 ($^{*}P < .05$; $^{**}P < .01$; $^{***}P < .001$, $^{****}P < .001$) were considered statistically significant.

Results

Long-term Culture of Pig Foliate Taste Epithelium in LGR4/6 Promoting Media Generates Taste Organoids

The FP were dissected from postmortem pig tongue, further dissected into ~1 mm^2 pieces, and digested using Collagenase P containing digestion media (Fig. 1A). The tissue digestion was washed and filtered through a 100 µm filter (to include single cells and small tissue/cell clumps) and plated using BME, thus giving rise to small reticulate taste organoids within 2 days in the LPM. Organoids in passage 0 (P.0) originated from both single cells and small cell/tissue clumps. Established organoids were passaged approximately every 14 to 15 days, and at the time of writing the maximum number of passages reached was 18. The taste organoids typically grew into multiple dense (reticulate) or cystic structures in culture, exhibiting organoid-within-organoid and budding organoid morphologies that could be observed by hematoxylin and eosin (H&E) staining (Fig. 1B). It has been routinely possible to cryopreserve and then thaw and expand the cells to generate new organoids.

Immunofluorescence (IF) and H&E staining of early passages (0-2) revealed a proliferating stratified outer cell layer positive for the marker of proliferation Ki67 that enclosed mature differentiated TRCs as marked by TRPM5 (26) (Fig. 1C) present in all sweet, bitter, and umami transducing TRCs and the epithelial cell marker CK13 (27) (Fig. 1C). Beyond passage 1 (P1), organoids were grown selectively from single cells and showed exponential growth in terms of average cell counts until day 16 and gradually plateaued thereafter (Fig. 1D). The dynamic growth and expansion of these organoids was recorded in real-time under brightfield from day 5 to 15 [Supplementary Video S1 (28)]. To gain insight into the types of cells present, we performed scRNA-Seq on dissociated organoid cells harvested at day 14 post-plating, prior to

Downloaded from https://academic.oup.com/endo/article/166/9/bqaf126/8221664 by Odense Universitetsbibliotek user on 21 April 2026

Table 2. Assignment of cell types to the clusters shown in the UMAP in Fig. 1E

Cluster #	Cell type	Genes
0	Basal epithelial cell	NGFR, TP63, PDPN[a], KRT5, KRT15, KRT17
1	Progenitor cell	KRT20, tyrosine kinase signaling
2	Precursor cell	STC1, CD68, CD24, SEMA3C, WNT7B, NGF, NECTIN, GJB3, CAV1, ZYX, SFN, ITGA6, CAPG, S100A14, PLP2, S100A10, DUSP7, NECTIN1
3	Cycling basal cell	H2AZ1, CDC20, TPX2, STMN1, PCLAF, glycolysis associated genes
4	Mesenchymal cell/fibroblast	PRRX1, mitochondrial genes
5	Cycling basal cell	TOP2A, PIF1, CDCA2, PLK1, HJURP, BUB1B, CDCA8, KIF11, IQGAP3, NDC80, KIF15, ASPM, ANLN, KIF18B, DIAPH3, KIFC1, KIF4A, DEPDC1, KIF2C, KIF20A, GTSE1, CEP55, DLGAP5, PCNA
6	Secretory cell airway epithelium/ ciliated cell	KRT4, SLP1, SLC6A14, WFDC2, MMP7, MMP15, SEM3A 80 genes associated with cytokine signaling in the immune system
7	TRC precursor	KRT20, NPY, SHH, IGF1, IRS1, TPH1, SEMA4A, SEMA7A, SOX2, NOTUM
8	Epithelial 1	MACC1, DSC2, TJP2, KCNMA1,
9	Epithelial 2	KRT18, IFNGR, IL6R
10	Epithelial 3	KRT4, GPR15LG, FGFBP1, KRT4, LYPD3, ADH7, AQP3
11	TRC	POU2F3, GNAT3, TRPM5, CCK, CALHM3

Abbreviation: TRC, taste receptor cell.
[a]PDPN NGFR, TP63- assignment from (29).

culmination of proliferation seen in Fig. 1D, to capture a broader spectrum of both proliferating and differentiated cell types. Figure 1E shows the UMAP (res = 0.5) with 12 distinct clusters representing proliferating basal cells (clusters 0-3 and 5), mesenchymal cells (cluster 4), epithelial cells (clusters 8-10), airway secretory cells (cluster 6), taste precursor cells (cluster 7), and a distinct cluster of cells expressing markers characteristic of TRCs (cluster 11); see Table 2 for marker genes used for cluster assignment. A heatmap displaying the top 5 genes per cluster can be found in Supplementary Fig. S1A (30). The marker genes for each cluster can be found in Supplementary Table S2 (31).

Using poly(A) enriched RNA-Seq, we compared the transcriptomic profiles of P1 organoids (day 14) with the paired foliate tissue of origin (n = 5). PCA of gene expression data revealed separate clustering of organoid and foliate samples with the first 3 principal components capturing 67.76% of the total variation (Fig. 1F). The transcriptomic profile of the taste organoids also revealed the expression of type I (*ENTPD2*), type II (*T1Rs*, *T2Rs*, *GNAT3, PLCβ2, TRPM5/4, CALHM1*), and type III markers (*OTOP1, SNAP25, NCAMs, PKD2L1*); see Table 3 for an outline of the main stem and TRC markers. Differential gene expression analysis of poly(A) enriched RNA-Seq (organoids vs foliate tissue) revealed a total of 8932 DEGs (false discovery rate < 0.05 and | log 2-fold change|>1), where 2396 genes are upregulated while 6536 are downregulated in the organoids (Fig. 1G). The top 100 most significant DEGs can be found in Supplementary Table S3 (43). Stem cell markers such as *LGR6, LGR4,* and *SOX2* (7, 8, 44) and the mature TRC marker *KCNQ1* were upregulated in the organoids compared to native tissue. IPA (Qiagen) of the DEGs (organoids vs foliate tissue) revealed significant enrichment of pathways such as PI3 K/AKT, GABAergic receptor, WNT/β-catenin (-log(*P*-value) = 7.01; Z-ratio = 0.611), BMP, insulin receptor, TGF-β ,and IGF-1 signaling [Supplementary Fig. S1B and S1C (30)] upregulated in the organoids, all of which have been described to have prominent roles in the development of the lingual epithelium, taste papillae, and taste bud function (45-47). GSEA of the DEGs revealed enrichment of signaling pathways such as mTORC, MAPK, and epidermal growth factor receptor/RAS/ERK that are heavily involved in G-protein coupled taste receptor signaling. Furthermore, gene sets involved in cell cycle activities such as DNA synthesis/replication and mitotic G1 to S transition are also enriched in the organoids [Supplementary Fig. S1D (30)], indicating their ability to further expand while also spontaneously differentiating into mature TRCs. We confirmed the presence of taste stem cell markers and mature TRC markers by qRT-PCR (Fig. 1H). Transcript levels of the taste progenitor cell markers *LGR6*, *LGR4,* and *SOX2* were significantly upregulated in the pig foliate taste organoids ($P < .05$; n = 3) when compared to the native tissue (Fig. 1H). Mature organoids also expressed transcripts for TRC markers *ENTPD2, GNAT3* (bitter, sweet, and umami transducing), *OTOP1* [sour transducing (38)], and *KCNQ1* (general mature TRC marker). Except for *ENTPD2*, these mature TRC markers also showed significant upregulation ($P < .05$) in the taste organoids relative to native tissue (Fig. 1H). Overall, this establishes for the first time that it is possible to propagate taste organoids from pig lingual tissue and that these organoids recapitulate the cellular format of the tissue of origin expressing both stem cell and mature TRC markers. The organoids reach a maximum growth expansion within 15 days post-initial plating, which is slower than that reported for mice (48), which is 6 days. Interestingly, pig fungiform papillae both in situ and in their representative organoids express predominantly *LGR4* and *LGR6* but not *LGR5;* unlike mouse taste organoids (49) but like mouse taste organoids, they express high levels of the taste stem cells specific factor *SOX2*.

Growth Factors SHH, FGF10, Wnt3a, RSO2, Noggin and Small Molecules CHIR99021, PGE2 Are Necessary for Optimal Growth and Differentiation of Taste Organoids

To determine the growth factors necessary for taste organoid development, SHH, FGF10, Wnt3a, RSO2, Noggin,

Downloaded from https://academic.oup.com/endo/article/166/9/bqaf126/8221664 by Odense Universitetsbibliotek user on 21 April 2026

Table 3. Native taste tissue and taste organoids are comprised of type I, type II, type III cells, bipotent stem cells, taste stem cells, and non-taste epithelium

Taste papillae cell type	Function	Marker gene
TRC	Cytokeratin 20 is a marker of TRCs (26, 32, 33), Voltage-gated potassium channel is a marker of mammalian taste buds of mouse, rat, and human KCNQ1 (34).	KCNQ1, CK20
Type I	Resemble astrocytes, which envelop other cell types, distinguished by the presence of the enzyme ectonucleoside triphosphate diphosphohydrolase 2, which breaks down adenosine triphosphate, a key neurotransmitter for type II TRCs (35).	ENTPD2
Type II	Long spindle-shaped cells that can sense bitter, sweet, and umami tastants through G protein-coupled taste receptors.	GNAT3 (36), TRPM5 (37),
Type III	Elongated, spindle-shaped cells with direct synaptic connections to afferent nerve fibers. These cells can sense sour taste.	OTOP1 (38)
Stem cells	Somatic stem cells, G-protein-coupled receptors LGR4/5/6-positive regulators of WNT signaling that give rise to taste stem cells. (7). Polycomb complex protein BMI1 in mice is an apparent marker of stem cells that only differentiate into epithelial cells (39).	LGR4, LGR5, LGR6, BMI1
Bipotent stem cells	Progenitor cells in the base of the taste bud. Give rise to both the non-taste lingual epithelium and the TRCs.	SOX2 (8, 40), CK14 (41)
Non-taste epithelium	Postmitotic lingual epithelium.	CK13 (42)

Identification of these cell types was done using established markers. Taste cell types were identified via the expression of cytokeratin 20 and potassium voltage-gated channel subfamily Q member 1 previously shown to label all mammalian TRCs. Subtypes of TRCs were identified by ectonucleoside triphosphate diphosphohydrolase, G protein subunit α transducin 3, transient receptor potential cation channel 5, or otopetrin 1. Stem cell markers used were cytokeratin 14, B cell-specific Moloney murine leukemia virus integration site 1, SRY-box 2, leucine-rich repeat-containing G-protein coupled receptor LGR4/5/6 marker genes, while cytokeratin 13 is a marker of mature epithelial cells.
Abbreviation: TRC, taste receptor cell.

CHIR99021, and PGE2, previously demonstrated to be essential for the long-term support of organoid growth (50-52), were systematically withdrawn from the media used to cultivate the organoids at the start of P3. Withdrawal of either of the individual factors Wnt3a/Rspo2/CHIR99021/Noggin/PGE2 caused a significant ($P < .001$) decrease in the expression of *LGR6* (Fig. 2A), while the withdrawal of FGF10 caused a significant ($P < .001$) increase. *SOX2* was significantly ($P < .001$) downregulated in the media that lacked Rspo2/CHIR/Noggin. However, the withdrawal of PGE2 from LPM significantly ($P < .01$) upregulated *SOX2* expression (Fig. 2A). In terms of mature TRC marker expression, the withdrawal of Noggin/PGE2 resulted in the significant ($P < .05$) downregulation of *KCNQ1* expression, although a significant increase ($P < .01$) in *GNAT3* expression was observed in the LPM (-) PGE2 media. Withdrawal of either of the factors Rspo2/CHIR99021/Noggin/PGE2 led to significant downregulation of *ENTPD2* expression ($P < .001$). Furthermore, removal of CHIR99021/Noggin from LPM significantly ($P < .01$) decreased the expression of *GNAT3* (Fig. 2B).

The most dramatic differences in culture morphology (under brightfield microscopy) were observed in the absence of either Noggin, CHIR99021, Rspo2, or Wnt3a (Fig. 2C). Withdrawal of either 1 of these factors yielded small, reticulate organoids with jagged edges, while the withdrawal of CHIR99021 gave rise to large, dense, reticulate organoids (compared to LPM). Removing Rspo2 from LPM yielded more cystic organoids, while the withdrawal of Wnt3a gave rise to more reticulate organoids similar in size to those grown in LPM (Fig. 2C). The efficacy of Rspo1, 2, or 3 in upregulating taste stem cell, taste progenitor cell, or TRC marker expression was tested using gene expression analysis of parallel cultures grown in LPM containing either Rspo1, 2, or 3. Rspo2 significantly ($P < .05$) upregulated *LGR6* expression over Rspo1, while a significant increase in insulin expression was observed in organoids grown in Rspo1 compared to Rspo3 [Supplementary Fig. S2A and S2B (30)]. No significant difference in the expression of TRC markers could be observed between the organoids grown in the presence of different R-spondins. Morphologically, the presence of Rspo2 in LPM resulted in larger organoids (with a mixture of cystic and reticulate structures) in denser cultures, compared to Rspo1 and 3 [Supplementary Fig. S2C (30)]. The effect of passaging on the expression of stem cell and TRC markers in the taste organoids was examined by comparing P2 and P10 cultures of the same taste organoid line. Expression levels of *LGR6* and *SOX2* were significantly decreased in the higher passage organoids. *LGR4,* however, maintained its expression level between P2 and 10 [Supplementary Fig. S3A (30)]. A significant decrease in the expression of TRC markers could be observed with the increase in passage number [Supplementary Fig. S3B (30)]. Thus, pig taste fungiform papillae organoids exhibit many of the growth factor dependencies observed in organoids grown from somatic stem cells from other organoids such as intestinal and mucosal organoids (50, 52).

Optimization of Culture Conditions to Upregulate the Expression of Mature TRC Markers

Cytokeratin 20 (CK20) is a known marker protein for human taste bud cells (32); similarly, here we show that taste organoids grown in LPM contain mature TRCs positive for CK20 (Fig. 3A, left: brightfield, right: immunofluorescence for CK20). Single cells from established porcine cell lines were cultured using a low shear stress, dynamic suspension, culture system at 37 °C in LPM (53). Like static cultures, the dynamic

Downloaded from https://academic.oup.com/endo/article/166/9/bqaf126/8221664 by Odense Universitetsbibliotek user on 21 April 2026

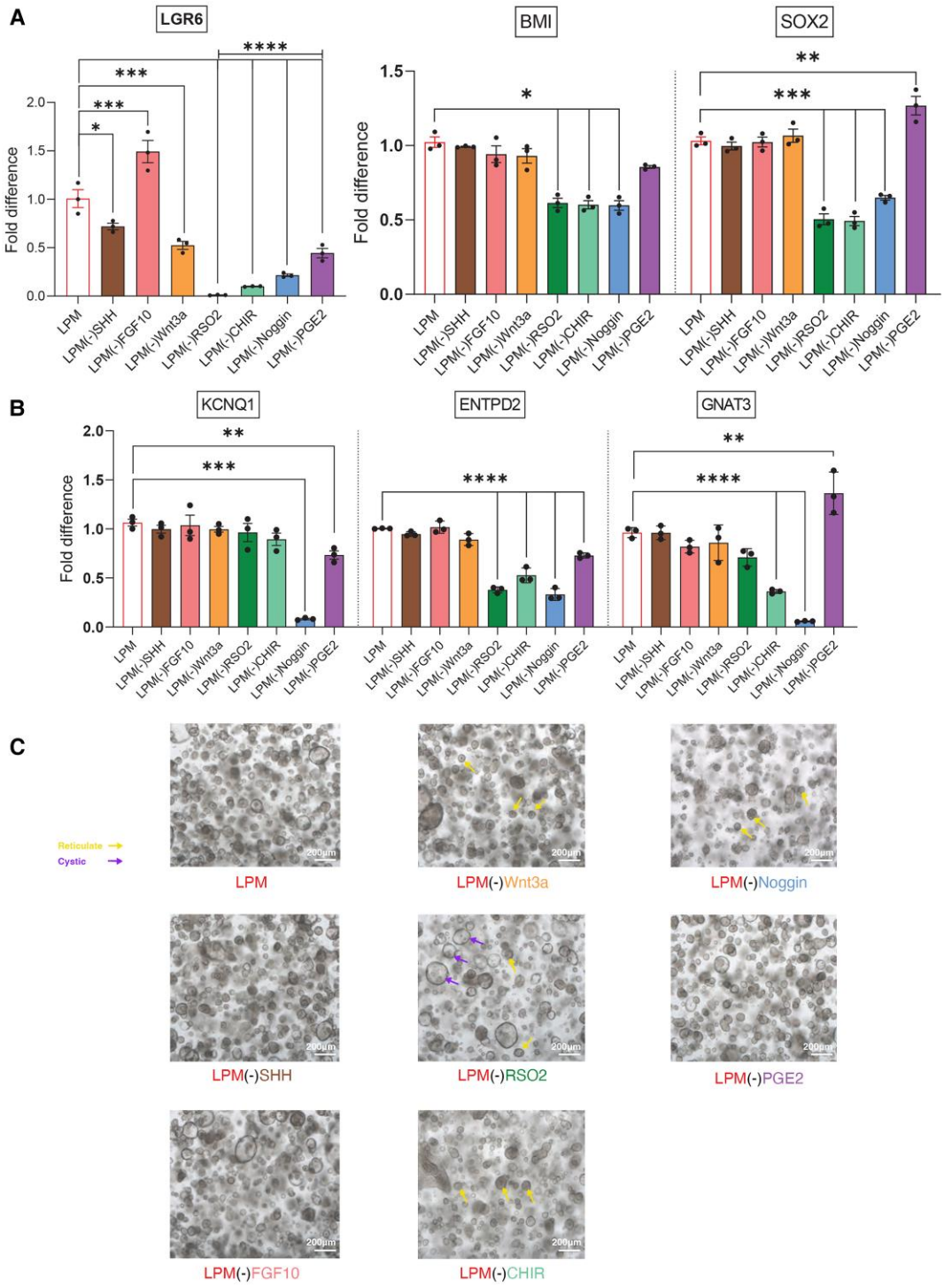


Figure 2. Effect of growth factor withdrawal on growth and/or differentiation of porcine taste organoids. (A) Expression of stem cell markers after growth factor withdrawal from LPM. Withdrawal of SHH, Wnt3a, RSO2, CHIR99021, Noggin, and PGE2 significantly decreased the expression of *LGR6*, while withdrawal of FGF10 significantly increased its expression. The expression of *BMI* and *SOX2* was significantly decreased by the withdrawal of RSO2, CHIR99021, and Noggin, while withdrawal of PGE2 significantly increased the expression of *SOX2*. (B) The expression of type I TRC marker *ENTPD2* was significantly decreased by the withdrawal of RSO2, CHIR99021, Noggin, and PGE2. The expression of *GNAT3*, a type II TRC marker, demonstrated decreased expression when RSO2, CHIR99021, and Noggin were removed from LPM. When PGE2 was removed, however, *GNAT3* expression was significantly increased, n = 3. (C) Representative brightfield images of taste organoids grown in LPM and in LPM with each factor withdrawn. The withdrawal of Noggin created the most noticeable morphological difference, giving rise to sparse organoid cultures and irregular-shaped small organoids, compared to LPM. The withdrawal of RSO2 gave rise to cultures with a higher abundance of cystic organoids, while LPM(-)CHIR9902 cultures had a higher abundance of reticulate organoids. Yellow arrows indicate examples of small reticulate organoids; purple arrows indicate examples of large cystic organoids. Data are presented as mean ± SEM; n = 3. **** $P < .0001$, *** $P < .001$, ** $P < .01$, * $P < .05$. *P*-values calculated using ANOVA. Scale bar, 200 µm.

Abbreviations:FGF10, fibroblast growth factor 10; LPM, Lgr4/6 promoting medium; PGE2, prostaglandin E2; RSO2, R-spondin-2; SHH, human sonic hedgehog; TRC, taste receptor cell; Wnt3a, wingless-related integration site 3A.

Downloaded from https://academic.oup.com/endo/article/166/9/bqaf126/8221664 by Odense Universitetsbibliotek user on 21 April 2026

cultures also produced organoids (Fig. 3B, right: brightfield image, left: H&E) by day 14 in culture.

Dynamic suspension culture organoids were positive for CK13 and CK14, which are markers for postmitotic epithelial, and bipotent stem cells, respectively (54) and for the TRC marker CK20 (Fig. 3C). However, dynamic culture led to a shift in the transcript levels of the somatic stem cell markers, with *LGR4* being the most prominent stem cell marker in static cultures whereas in dynamic cultures *LGR6* was most prominent (Fig. 3D). *LGR6* expression in dynamic cultures had a multifold increase over comparable static cultures while the inverse was observed for the expression of *LGR4* (Fig. 3E). Although not statistically significant, there was increased expression of the taste progenitor cell marker *SOX2* in the static cultures compared to dynamic cultures (Fig. 3E). The expression of mature TRC markers *GNAT3*, *TRPM5*, and *OTOP1* were significantly upregulated ($P < .05$; $n = 3$) in the taste organoids grown in dynamic culture vs static culture (Fig. 3F).

While spontaneous differentiation into TRCs was observed in organoids grown in LPM, we further tested 8 different media formulations for improved taste organoid differentiation using parallel organoid cultures as indicated in Supplementary Fig. S3C (30). Based on the expression of TRC marker genes and morphological characteristics [Supplementary Fig. S3C and S3D (30)], media C5 was selected to conduct subsequent differentiation experiments. C5 media was formulated by removing growth factors Wnt3a, SHH, nicotinamide, CHIR99021, A8301, and SB202190 from LPM and adding IGF1, IGF2, exendin-4 (a GLP-1 receptor agonist), DAPT (γ-secretase inhibitor), and interleukin 22 to promote differentiation and enhanced expression of transcripts for TRC marker genes. Established organoid cultures were fed with LPM from days 0 to 10 and then transferred to the C5 medium and harvested on day 16 (C5 organoids), while a parallel culture was maintained in LPM for the same duration (LPM organoids) for comparison. C5 organoids exhibited significant upregulation of all mature TRC markers while the expression of *LGR6* was significantly downregulated (Fig. 3G). The expression of *SOX2,* however, was not different between LPM and C5 organoids. LPM and C5 organoid cultures, by brightfield, showed significant differences in their morphology in that, at day 16, C5 organoids were smaller, denser, and reticulated in nature compared to LPM organoids that maintained their typical morphology of a mix of cystic and reticulate organoids that were more circular and uniform in shape (Fig. 3H).

IGF1/IGF2 signaling is necessary for the maintenance of *LGR6/SOX2* expression and hence for the growth and differentiation of foliate taste organoids.

As we observed in mouse and human taste buds (11), insulin protein is present in pig taste buds within taste papillae (Fig. 4A). Pig insulin was extracted from taste papillae (CVP, Fig. 4A, top panel) by classic acid-ethanol extraction and when CHO-IR cells (55) were serum starved for 5 hours and treated with the extracted insulin for 5 minutes (Fig. 4A, top panel), phosphorylation of the insulin receptor (pIR-β, Tyr1162/1163) and the activation of the downstream signaling proteins IRS1/2 (pIRS1/2 Tyr612) and pAkt (Ser473) occurred only in the CHO-IR cells (Fig. 4A, bottom left). As a control, CHO cells were treated with human insulin (10 nM), in which no activation of pIR(Tyr1162/1163) or p-Akt(Ser473) was observed [Supplementary Fig. S4A (30)]. This establishes the existence of biologically active insulin in pig taste papillae. Insulin was also shown to be present by immunofluorescent staining (Fig. 4A, bottom right panel).

Having now shown that pigs in addition to mice, rats, and humans produce biologically active insulin in type II TRCs in posterior papillae, we wanted to decipher the importance of insulin in the growth and differentiation of our pig taste organoids. Increasing the concentration of insulin was previously shown to have a detrimental effect on the growth and differentiation of mouse taste organoids (56); hence LPM was formulated using insulin-free supplements, thus enabling us to investigate the effects of insulin, IGF1, and IGF2, when added individually, to pig taste organoids. Supplementing LPM with a minimum of 10 nM human insulin was essential for the proper growth of the taste organoids as evident in the brightfield images of organoid cultures in increasing insulin concentration from 0 to 50 nM (Fig. 4B). In contrast to the work described on mouse taste organoids, increased concentrations of insulin did not show any morphologically detrimental effect on the organoids under the brightfield microscope. In fact, higher concentrations of insulin resulted in denser organoid cultures with a higher number of reticulate organoids (Fig. 4B). The necessity of insulin for the proper growth of the taste organoids is further affirmed by the statistically significant multifold increase observed in transcript levels of *LGR6* and *SOX2* ($P < .001$ and $P < .05$, respectively) in organoid cultures grown in >10 nM insulin. Supplementing culture media with insulin (>10 nM) also upregulated the expression of mature taste cell markers in a concentration-dependent manner, without affecting levels of *BMI1* (Fig. 4C), a transcript associated with epithelial cell progenitors (57). Substitution of insulin with IGF1 or IGF2 did not yield morphological differences in comparative organoid cultures (Fig. 4D). In terms of the upregulation of taste stem cell markers and mature TRC markers, LPM supplemented with IGF2 performed better than LPM supplemented with IGF1, particularly at the 20 and 50 ng/mL concentrations. IGF1, however, significantly increased BMI1 expression compared to IGF2 in comparable cultures under different concentrations spanning 0 to 50 nM (Fig. 4E). Thus, we have demonstrated that insulin/IGF signaling is necessary for the growth and differentiation of taste organoids, a fact that has been in contention (56).

Differentiation of Taste Organoids into Insulin -producing Structures

Taste organoids grown in LPM harvested on day 14 and beyond exhibited expression of marker genes for mature TRCs—*ENTPD2, GNAT3*, and *OTOP1*—indicating the presence of types I, II, and III TRCs, respectively (as described earlier). Moreover, we detected insulin protein in these organoids by IF as depicted in Fig. 5A, where a subset of mature CK20-positive TRCs co-stain for insulin. As complementary evidence (depicted in Fig. 5B), we detected the expression of transcripts for insulin and 2 of its critical transcription factors, *PAX4* (58) and *MAFA* (59), both in mature taste organoids and in pig native tissue. Although not statistically significant, organoids grown in LPM in dynamic culture had increased expression of insulin and its essential transcription factors (*PAX4* and *MAFA*) compared to static LPM cultures (Fig. 5C).

Downloaded from https://academic.oup.com/endo/article/166/9/bqaf126/8221664 by Odense Universitetsbibliotek user on 21 April 2026

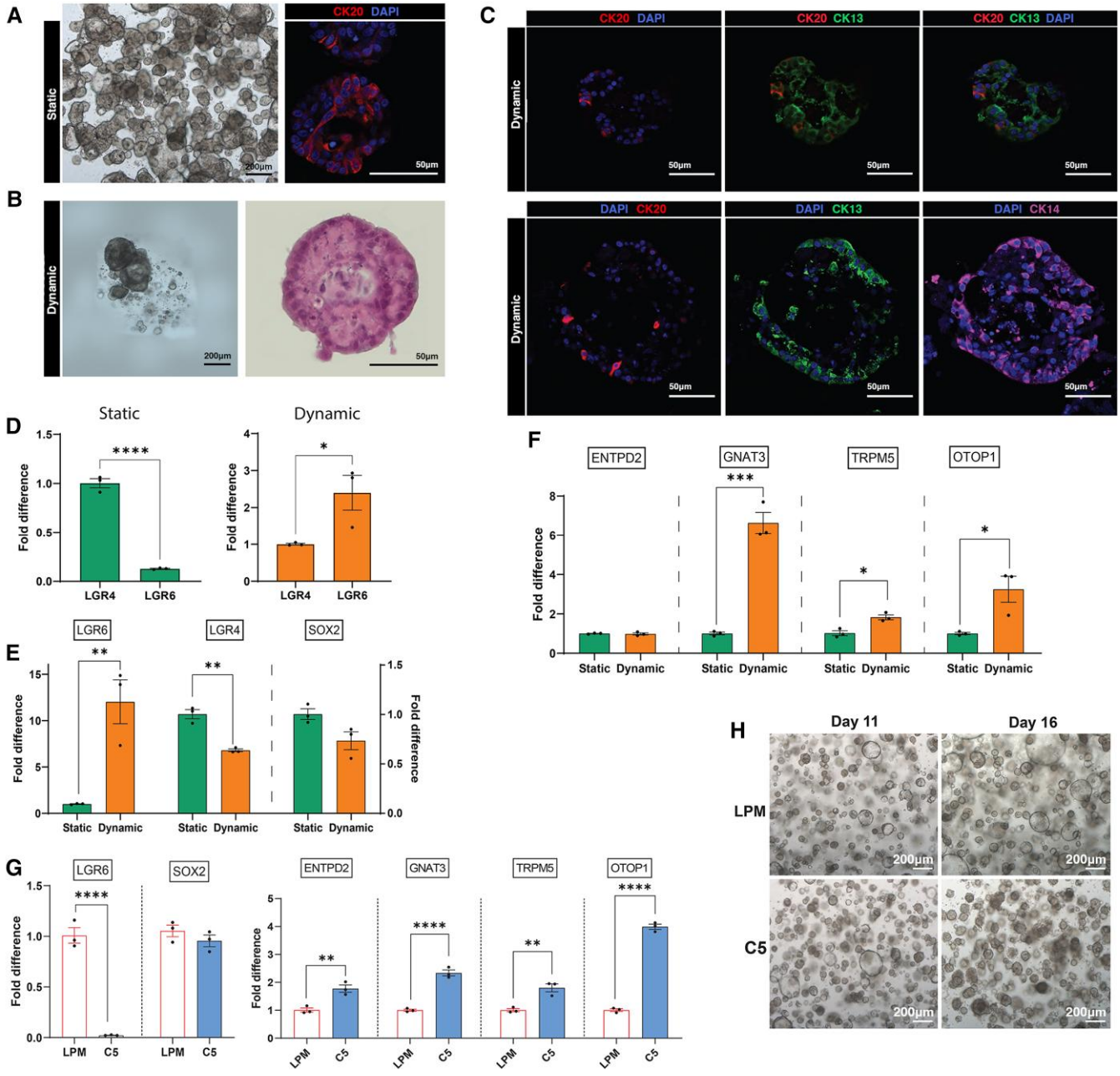


Figure 3. C5 media and dynamic culture in simulated microgravity alter stem cell marker expression and upregulate TRC marker expression. (A) Brightfield microscopy images of taste organoids (scale bar: 200 μm) grown using static culture (left) and their immunofluorescence staining (right) depicting CK20$^+$ mature taste cells are shown in red; nuclei stained for 4′,6-diamidino-2-phenylindole dihydrochloride are shown in blue (scale bar: 50 μm). (B) Brightfield microscopy images of taste organoids grown in dynamic culture on the left (scale bar: 200 um) and their typical morphology depicted via hematoxylin and eosin staining on the right (scale bar: 50 μm). (C) Immunofluorescence staining of taste organoids grown in dynamic culture, showing the existence of mature taste cells (CK20) and the taste epithelium (CK13 keratinocytes). Scale bar: 50 μm. (D) Expression of stem cell markers *LGR4* and *LGR6* in static and dynamic cultures. *LGR4* is the prominent stem cell marker in static cultures; in dynamic cultures, however, *LGR6* expression is prominent over *LGR4* (n = 3). (E) Quantitative RT-PCR data depicting the comparison of taste progenitor cell marker (*SOX2*), stem cell marker (*LGR4* and *LGR6*), and mature taste cell marker expression in static vs dynamic cultures. *LGR6* expression in dynamic cultures was significantly higher than comparable static cultures, while *LGR4* expression was significantly higher in the static cultures. No significant difference in the *SOX2* expression was observed (n = 3). (F) Dynamic culture of taste organoids upregulates TRC marker gene expression. Organoids grown in dynamic cultures showed significant upregulation in type II (*GNAT3, TRPM5*) and type III (*OTOP1*) TRC markers, although no significant difference in type I marker *ENTPD2* was observed (n = 3). (G) Comparative expression of stem cell markers (*LGR6, SOX2*) and mature taste cell markers (*ENTPD2, GNAT3, TRPM5, OTOP1*) in organoids that were transferred to C5 (differentiation media) on day 11 and harvested at day 16 compared to organoids that were grown LPM throughout (day 0 to day 16). C5 media appear to significantly downregulate the expression of *LGR6* and significantly upregulate the expression of all mature TRC markers. No significant difference could be observed in *SOX2* expression (n = 3). (H) Brightfield images (at day 11 and day 16) of taste organoids grown in LPM (day 0 to day 16) and of a parallel culture that was transferred to C5 media at day 11. The C5 organoids appear to be smaller and denser reticulate structures by day 16, compared to LPM organoids of similar age. Scale bar: 200 μm. Data are presented as mean ± SEM. *P*-values calculated using ANOVA. **** $P < .0001$, *** $P < .001$, ** $P < .01$, * $P < .05$.

Abbreviations: CK20, cytokeratin 20; LPM, Lgr4/6 promoting medium; TRC, taste receptor cell.

Downloaded from https://academic.oup.com/endo/article/166/9/bqaf126/8221664 by Odense Universitetsbibliotek user on 21 April 2026

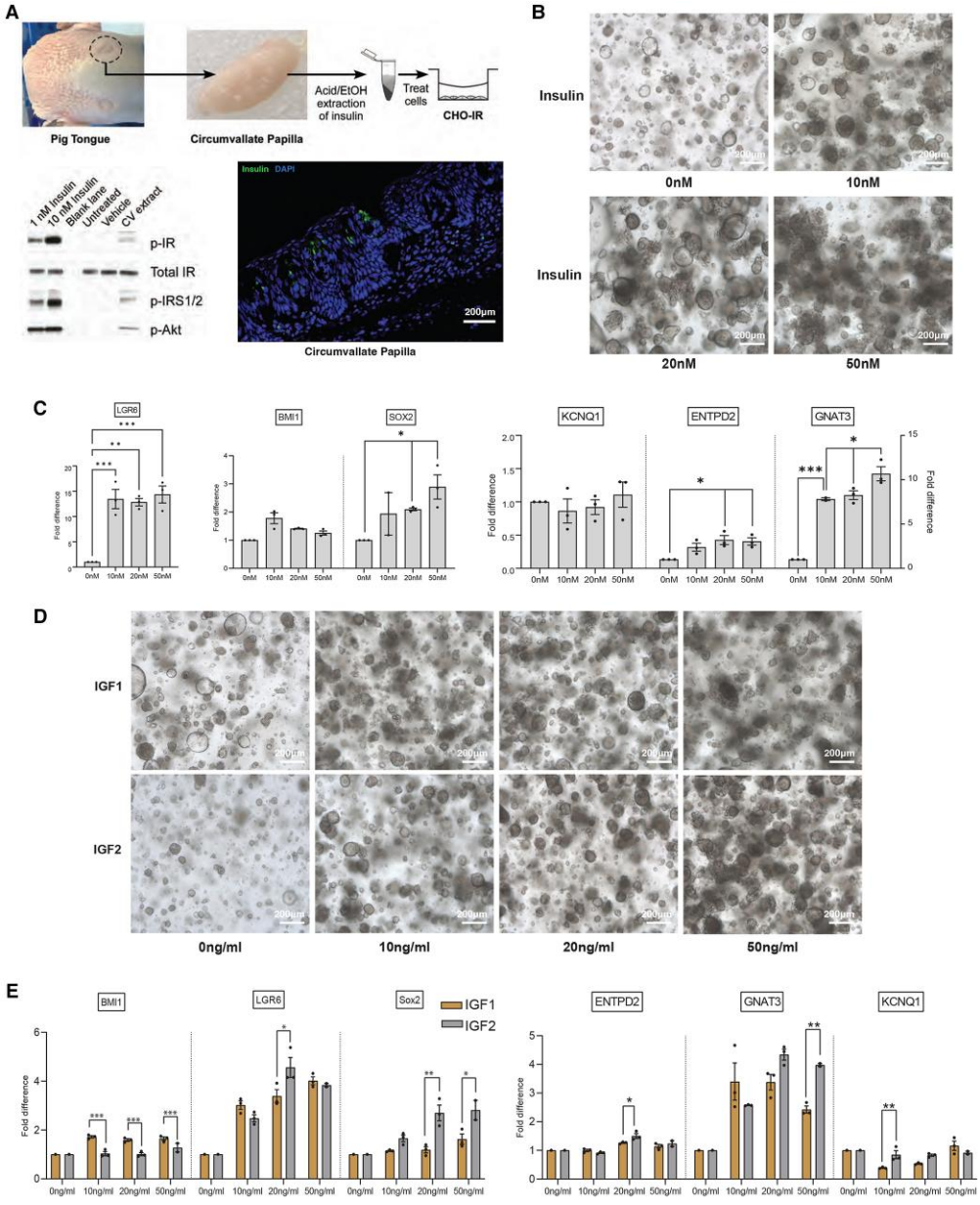


Figure 4. IGF1/IGF2 signaling is necessary for growth, expansion, and differentiation of porcine taste organoids. (A) Insulin is present in pig taste papillae. Top panel outlines the process of acid/ethanol extraction of insulin from pig CV and its activation of the insulin receptor in CHO-IR cells. Bottom left panel shows an immunoblot of extracts from CHO-IR cells treated with human insulin, vehicle (water), and pig CV papillae acid/ethanol extract. Bottom right panel shows pig CV insulin immunostaining. (B) Representative bright field images of taste organoids (day 16) grown in LPM, with increasing insulin concentrations. Organoid cultures grown with no insulin in LPM were observed to have the lowest density and the highest number of cystic structures. Organoid cultures grown in LPM with >10 nM insulin were denser and more reticulate in structure. Increasing organoid density could be observed with increasing concentrations of insulin in LPM. (C) Gene expression analysis of epithelial stem cell, taste stem cell, and mature taste markers in taste organoids (harvested on day 16) grown in LPM with increasing concentrations of insulin. The expression of LGR6 was significantly higher in LPM (>10 nM insulin) cultures vs LPM (0 nM insulin). The expression of *SOX2* follows the same trend with the highest statistically significant expression at 50 nM insulin. The highest expression of *BMI1* was observed at 10 nM insulin. Both type I (*ENTPD2*) and type II (*GNAT3*) taste cell marker expression significantly increased in an insulin concentration-dependent manner with the highest expression at 50 nM insulin in LPM. Transcript levels of *KCNQ1* were not affected by the insulin concentration in LPM (n = 3). (D) Representative brightfield images of organoid cultures (day 16) grown in LPM in which insulin was substituted with increasing concentrations of either IGF1 or IGF2 [LPM (IGF1/IGF2)]. Organoid cultures in LPM (>10 ng/mL IGF1/IGF2) had a high density of mostly reticulate organoids vs organoid cultures in LPM (0 ng/mL IGF1/IGF2) that were sparser and more cystic in nature. The densest cultures were observed at 50 ng/mL IGF1/IGF2. (E) Expression of stem cell and mature taste cell markers in increasing concentrations of LPM (IGF1/IGF2). For both LPM (IGF1) and LPM (IGF2), expression of both *LGR6* and *SOX2* increased in a concentration-dependent manner with the highest expression at 20 ng/mL and 50 ng/mL, respectively. Organoids grown in LPM (IGF2) had significantly higher expression of both these markers vs LPM (IGF1) at these concentrations as well. For *BMI1,* however, organoids in LPM (IGF1) had significantly higher expression compared to LPM (IGF2) organoids in all concentrations >0 ng/mL. Both LPM (IGF1) and LPM (IGF2) organoids had higher expression of TRC markers compared to LPM (–) IGF1/IGF2. For *ENTPD2* and *GNAT3*, LPM (IGF2) organoids had significantly higher expression at 20 ng/mL and 50 ng/mL, respectively, whereas for KCNQ1 this was at 10 ng/mL of IGF2. n = 3; *P*-values calculated using ANOVA. Data are presented as mean ± SEM. *** $P < .001$, ** $P < .01$, * $P < .05$. Scale bar, 200 µm.

Abbreviation: CHO-IR, Chinese hamster ovary expressing the insulin receptor; CV, circumvallate tissue; IR, insulin receptor; LPM, Lgr4/6 promoting medium.

Downloaded from https://academic.oup.com/endo/article/166/9/bqaf126/8221664 by Odense Universitetsbibliotek user on 21 April 2026

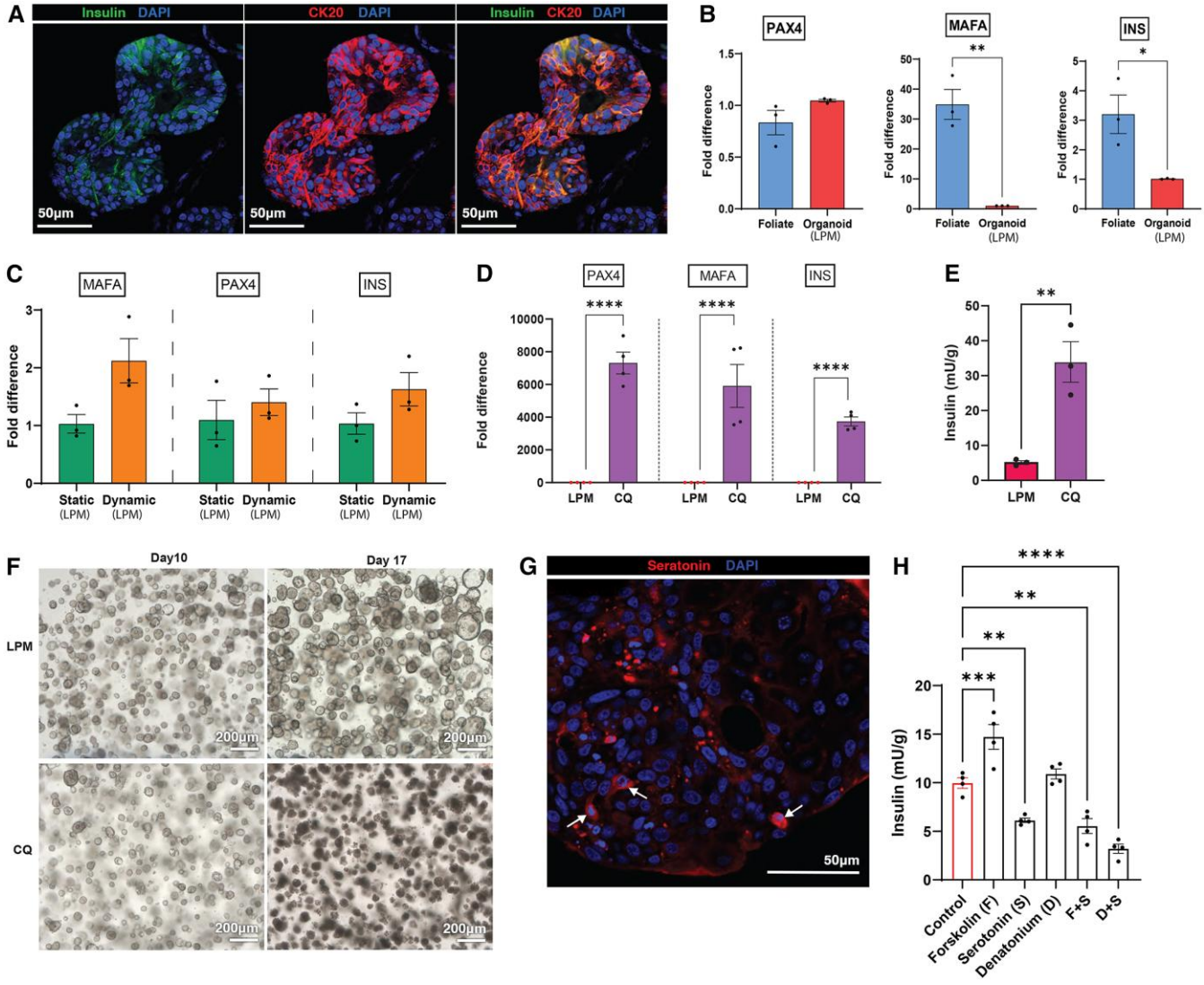


Figure 5. Improved insulin and insulin transcription factor expression in CQ media for taste organoids. (A) Insulin is produced in taste organoids. CK20 (red) and insulin (green) immunofluorescence staining on taste organoids grown in LPM, harvested on day 16. CK20 is a marker for mature TRCs. Note that only a subset of CK20 cells is co-stained with insulin, upholding our previous observation that only type II TRCs are capable of producing biologically active insulin. Scale bar, 50 µm. (B) Bar graphs depicting the quantitative RT-PCR data on the expression of insulin and insulin transcription factors (PAX4, MAFA) in porcine foliate taste organoids grown in LPM in comparison to native foliate tissue (n = 4; ie, tissue from 4 separate pigs and their corresponding organoids). (C) Quantitative RT-PCR data comparing the expression of insulin and its essential transcription factors, *MAFA* and *PAX4*, in static and dynamic cultures. Though not significant, dynamic cultures in LPM do appear to increase the expression of insulin, MAFA, and PAX4 in comparison to parallel static cultures in LPM (n = 3). (D) Bar graphs showing quantitative RT-PCR data comparing the expression of insulin and insulin transcription factors in organoids grown in LPM and CQ media. A multifold increase in the expression of insulin and its transcription factors could be observed in organoids grown in CQ media (n = 4). (E) Total insulin assayed using porcine insulin ELISA, produced in organoids grown in CQ, in comparison to organoids grown in LPM. CQ organoids produce a significantly higher amount of insulin protein in comparison to LPM organoids. Mean of 3 separate experiments (n = 3). (F) Brightfield microscope images of different organoid morphologies exhibited by organoid cultures grown (parallel) in LPM (from day 0 to day 17) and in CQ media (day 0 to day 10 in LPM, day 10 to day 17 in CQ). A stark difference in the organoid morphologies could be observed in LPM and CQ cultures at day 17, where CQ organoids appear as dark, dense structures. Scale bar, 200 µm. (G) Serotonin immunofluorescence staining (red) of mature taste organoids providing clear evidence of serotonin produced in the taste organoids. Scale bar, 50 µm. (H) Total insulin measured using porcine insulin ELISA, produced in mature taste organoids grown in LPM and treated overnight with forskolin (1 µM), serotonin (5 µM), denatonium (1 mM), forskolin + serotonin, denatonium + serotonin. Overnight treatment with forskolin significantly increased insulin production, while serotonin treatment reduced its production. Treating with denatonium did not yield any significant difference in the total insulin produced. When forskolin or denatonium was combined with serotonin, there was a significant reduction in the total insulin production (n = 3). Values presented as mean ± SEM. *P*-values calculated using ANOVA. **** $P < .0001$, *** $P < .001$, ** $P < .01$, * $P < .05$.

Abbreviations: CQ, quiescence condition; LPM, Lgr4/6 promoting medium; TRC, taste receptor cell.

Due to the potential utility of pig taste organoids as a model to study lingual insulin production and function, we wanted to optimize insulin expression in the differentiated TRCs within the organoids. Inhibition of FOXO1 in intestinal organoid cells was used to enhance insulin expression through the upregulation of PDX-1 (60). The addition of the small molecule FOXO1 inhibitor AS1842856 to C5 (C5 + iFOXO1 media) resulted in significant upregulation of *LGR6* and *BMI1* and downregulated the expression of *SOX2* and *KCNQ1* in comparison to taste organoids grown in LPM. However, it

Downloaded from https://academic.oup.com/endo/article/166/9/bqaf126/8221664 by Odense Universitetsbibliotek user on 21 April 2026

(C5 + iFOXO1) did not impede the expression of insulin, *MAFA*, and *PAX4* compared to C5 organoids, which already exhibited a significant upregulation in *INS/MAFA/PAX4* expression compared to LPM organoids [Supplementary Fig. S4B (30)]. Next, we induced quiescence through the combined inhibition of epidermal growth factor receptor signaling, Wnt, Notch, and MAPK pathways using small molecule inhibitors of these pathways (61) [see Supplementary Table S4 (62) for details]. The CQ media is C5 without epidermal growth factor but with SCH772984, Mirdametinib, Afatinib, AZD-8055, and Gefitinib, IWP-2, and the FOXO1 inhibitor AS1842856 (note C5 media already has DAPT, a Notch inhibitor). The organoids were first grown in LPM, transferred to CQ media on day 10, and then harvested on day 16. Control samples were grown in LPM from days 0 to 16. Organoids transitioned into CQ media on day 10 and harvested on day 16 had more than a 3739-fold ±546 (n = 4) increase in the expression of insulin and its transcription factors *PAX4* (7312 ± 1338 fold; $P < .0001$; n = 4) and *MAFA* (5908 ± 2631 fold; $P < .0001$; n = 4) compared to control samples (Fig. 5D). CQ organoids also demonstrated significant upregulation of *SOX2* (26 ± 4 fold; $P < .0001$; n = 4) and *KCNQ1* (146 ± 20 fold; $P < .0001$; n = 4) expression [Supplementary Fig. S5A (30)].

To demonstrate that insulin is fully processed (transcribed and translated) in our taste organoids, we performed a pig-specific insulin ELISA on acid-ethanol insulin extractions from LPM and CQ organoids. When normalized to total protein, insulin content from CQ organoids was significantly increased (6.5 ± 0.5, fold, $P < 0.01$) relative to LPM (Fig. 5E). Distinct morphological differences could also be observed in the organoids treated with CQ media where they grew into small, dense, irregular-shaped structures without well-defined borders, in stark contrast to LPM grown (control) organoids (Fig. 5F). We further analyzed the transcriptomic profile of organoids grown in CQ media in comparison to LPM organoids using poly(A) enriched RNA-Seq data, which revealed clear heterogeneity in their gene expression. PCA of their transcriptomic profiles revealed separation of CQ and LPM samples into 2 clear clusters in 3D space [Supplementary Fig. S5B (30)]. Differential gene expression analysis (CQ vs LPM) revealed 3139 downregulated and 1830 upregulated genes in the CQ organoids compared to LPM (−log *P*-value >1.3 and |Log2FC|>1). Genes such as *MAFA, MAFB*, and *ONECUT1*(*HNF6*), which play pivotal roles in pancreatic development, β-cell function, insulin synthesis, and glucose metabolism, were significantly upregulated in CQ organoids (63-65). Serotonin receptors *HTR2B* and *HTR7* were also significantly upregulated in the CQ organoids, while *HTR6* was downregulated. *KCNQ1, GNAT3, SOX2*, and *LGR6* were downregulated in the CQ organoids [Supplementary Fig. S5C (30)]. Pathway enrichment analysis (using Qiagen IPA) of DEGs revealed upregulation of BMP signaling, P13/AKT signaling, insulin receptor signaling, GABAergic receptor signaling, p-53 signaling, and semaphoring interactions [Supplementary Fig. S5D (30)]. Cell signaling pathways such as Notch signaling, FGF and MAPK signaling, senescence pathways, and chromosomal replication were downregulated in CQ organoids [Supplementary Fig. S5E (30)].

We have found that insulin release is under regulatory control by serotonin in the choroid plexus (12), and we detected by IF the expression of serotonin in our mature taste organoids cultured in LPM (Fig. 5G). To determine how insulin synthesis is regulated in the taste organoids, we tested insulin production in pig taste organoids in response to a bitter taste stimulusdenatonium benzoate, a neurotransmitter serotonin, and as gustatory stimuli modulate cAMP, the second messenger signaling moiety (66), forskolin. As shown in Fig. 5H, mature organoids grown in LPM for 14 days were washed and treated overnight in DMEM/F12 supplemented with forskolin, serotonin, denatonium benzoate, forskolin + serotonin, and denatonium benzoate + serotonin. Total insulin content after overnight treatment was measured in acid-ethanol extractions using porcine insulin ELISA. Insulin content in the taste organoids that were treated with forskolin was significantly ($P < .001$) elevated, while it was significantly decreased in the serotonin-treated organoids ($P < .01$), compared to control (DMEM/F12 only). Furthermore, organoids treated with forskolin + serotonin and denatonium benzoate + serotonin both exhibited a significant decrease ($P < .005$) in insulin content compared to control. No significant difference in insulin could be detected in organoids treated with denatonium benzoate vs control. We did not detect any difference in the transcript levels of TRC markers, insulin, or insulin critical transcription factors in these treated organoids relevant to untreated controls [Supplementary Fig. S6A and 6B (30)]. We did detect the expression of serotonin receptors *HTR1D, HTR2A, HTR4,* or *HTR7*, the transcript levels of which were unaffected by the addition of the modulators or any combination thereof [Supplementary Fig. S6C (30)]. We found that *HTR1D* is the most highly expressed transcript in taste organoids cultured in LPM [Supplementary Fig. S6D (30)]. We also observed the expression of tryptophan hydroxylase (*TPH*) as a proxy for serotonin production [TPH1/2 are rate-limiting enzymes essential for the biosynthesis serotonin (67)] by qRT-PCR [Supplementary Fig. S6E) (30)] with *TPH2* being the most highly expressed enzyme. Transcript levels of either hydroxylase were not affected by the addition of serotonin, forskolin, or denatonium benzoate or combinations thereof [Supplementary Fig. S6F (30)]. Thus, we found by 3 different methods (qRT-PCR, immunostaining, and ELISA assay) that insulin is transcribed and translated in pig taste papillae organoids and that insulin in pig TRCs is biologically active and its production is stimulated by cAMP, a process likely subject to negative regulation by serotonin. Similar to the cells of the choroid plexus cells that make fully mature insulin but do not express PDX-1 (12), we would not expect insulin release from TRCs to be under glucose control.

Discussion

In this study we comprehensively characterized the cellular composition, growth, and differentiation of *LGR4/6* expressing taste organoids derived from pig foliate taste tissue. We optimized growth conditions for the organoids by systematically varying media components and monitored gene expression in organoids maintained and passaged long term so we could generate a taste organoid model that could be used by researchers. Initially, we grew 3D "organoid" structures from single cells/tissue clumps (P0) and then from single cells (P1 onwards) that contain both dividing cells (Ki67$^+$) and mature TRCs (eg, TRPM5$^+$, CK20$^+$). Furthermore, our taste organoids had upregulated expression of type II (*GNAT3*, *TRPM5*), and sour-detecting (*OTOP1*) TRC markers as well as stem (*LGR4/6*) and pluripotency/taste progenitor cell markers (*SOX2*) in comparison to the originating foliate

Downloaded from https://academic.oup.com/endo/article/166/9/bqaf126/8221664 by Odense Universitetsbibliotek user on 21 April 2026

tissue from which they were derived. Dynamic suspension culture increased expression of TRC transcripts, and dynamic and long-term culture produced organoids with a more homogeneous distribution of stem, epithelial, and TRCs lacking the apical-basal polarization observed in early passages. We show that insulin is essential for the growth and differentiation of taste stem cells and that IGF1/2 can substitute for insulin in maintaining a robust culture. We found by 3 different methods (qRT-PCR, immunostaining, and ELISA assay) that insulin in transcribed and translated in pig taste papillae and organoids. We tested methods of enhancing hormone production (61, 68), showing that inhibition of growth factors and induction of quiescence is extremely effective at increasing insulin transcription and translation in type II taste receptor cells, which are terminally differentiated cells. Lastly, we demonstrate that the insulin produced in TRCs is biologically active and its production is stimulated by cAMP, a process likely subject to negative regulation by serotonin. Indeed, expression of *HTR1A*, a G_i coupled G-protein coupled receptor, specifically in the insulin-producing type II taste cells of rats, was already reported in previous studies (69).

The LGR4/6 promoting media developed by us was primarily based on DMEM/F12 and conditioned by the addition of multiple growth factors comprising both small molecules and peptides previously shown to promote Wnt/β-catenin signaling (6) and to promote taste organoid formation in mice (7, 8, 45, 48, 49, 70). In accordance with the literature discussing both taste and non-taste organoids (7, 45, 71), growth factors such as Wnt3a, Rspo2, CHIR99021, Noggin, and PGE2 were essential in maintaining taste stem cells (*LGR6* expression) and for differentiation in our taste organoids. More specifically to taste organoids, SHH has been shown to be an upstream positive regulator of SOX2, and hedgehog signaling is required for TRC differentiation (8, 40). Removal of SHH from LPM did not significantly affect the density of organoid growth or the transcript levels of *SOX2* and TRC marker genes but did significantly reduce *LGR6* expression. This indicated SHH may be required for lingual stem cell maintenance but not for TRC differentiation. This agrees with observations in cultured mouse taste organoids where the addition of a Smoothened agonist in the differentiation phase did not increase TRC marker gene expression in SOX2 enriched organoids (8). Removal of FGF10 from LPM resulted in upregulation of *LGR6* expression but had no significant effects on TRC marker gene expression, which agrees with observations in the mouse that FGF10 controls the size of the progenitor field (72-74). Interestingly, the absence of PGE2 in the media appears to upregulate transcript levels of both *SOX2* and *GNAT3* while downregulating those of *LGR6* and *ENTPD2*. There are several reports that PGEs play an important role in stem cell maintenance/proliferation and enhancement of organoid formation (75-77). However, it is not clear whether PGE2 could be used to direct differentiation into specific TRC subtypes, which could be explored further in this organoid model.

Organoids that had only been passaged once and then harvested on day 14 had higher *LGR6* and *LGR4* transcript expression compared to the foliate tissue of origin. Of note, *LGR5* transcript expression was not detected by qRT-PCR in native foliate tissue or in any of our cultures, either static or dynamic. Gene expression profiling of our taste organoids, supported by both qRT-PCR and poly(A) enriched RNA-Seq data, indicates upregulated expression of mature TRC markers such as *KCNQ1, GNAT3,* and *OTOP1*. However, the expression of *ENTPD2*, a marker for type I TRCs, was significantly downregulated in the RNA-Seq data as well as having much lower expression in the qRT-PCR data compared to native taste tissue. This is possibly due to some remnant of muscle tissue being present on the foliate papilla. We chose to do scRNA-Seq analysis on day 14 of culture post-passaging to facilitate the capture of a broader spectrum of cell types inclusive of both proliferating and differentiating cells. This could account for the smaller cluster of cells that are enriched in TRC gene markers.

Rodent taste organoids have been shown to spontaneously differentiate into TRCs, which we also observed here with our pig taste organoids (7, 48, 49). In addition to removing growth factors as had been done previously with mouse taste organoids (8), we also tried 8 different media compositions with added differentiation factors to optimize expression of TRC marker transcript levels. We developed C5, a medium to enhance TRC marker transcript expression in differentiated organoids, which was clearly permissive to significantly upregulating all TRC markers as well as upregulating expression of insulin and its transcription factors while downregulating the expression, in general, of stem cell markers. When compared to organoids grown in LPM only, C5 organoids showed clear morphological differences under brightfield microscopy, where they were comparatively denser and reticulated.

Early passage taste organoids grown in static LPM culture exhibited a cellular organization that consisted of a stratified proliferating outer cell layer encompassing the mature TRCs in the middle. However, late passage organoids (in static LPM culture) contained mature TRCs dispersed throughout organoids, and the cells could be found both in the periphery and the center of organoids. This contrasts with what is previously described for murine-derived taste organoids; they had to be transferred into suspension culture to alter the apicobasal orientation of the organoids (70). The gene expression profile of early and late passage (P2 and P10) organoids from the same cell line also bore significant differences in terms of stem cell, taste progenitor, and TRC marker gene expression. These differences in self-organization and gene expression could be due to physiological differences that occur in organoid biology when a cell line undergoes continuous passaging. H&E staining of the organoids typically showed reticulate and cystic structures with budding and organoid-within-organoid morphologies.

The same pig cell line showed a marked difference in gene expression profiles when cultured in static and dynamic cell culture systems, with statistically significant upregulation in transcripts of mature TRC markers in dynamic cultures. Dynamic suspension culture of the organoids in LPM had improved stem cell marker (*LGR6*) and mature taste cell marker expression (*GNAT3, TRPM5, OTOP1*) compared to static LPM cultures. Insulin and its transcription factors were also upregulated in the dynamic culture. The most interesting difference from a stem cell perspective, however, was in the altered expression of LGRs in the dynamic culture system, in comparison to both static culture and native taste tissue. In taste organoids in dynamic culture, there was significant upregulation of *LGR4* compared to *LGR6* and compared to *LGR6* itself in the comparable static culture. Hence, the most highly expressed stem cell marker for the dynamic cultures was *LGR6,* but in static cultures it was *LGR4*. Thus, dynamic suspension culture might be the optimal culture system

Downloaded from https://academic.oup.com/endo/article/166/9/bqaf126/8221664 by Odense Universitetsbibliotek user on 21 April 2026

for maintaining both *LGR6* and TRC expression levels over long-term expansion in vitro. Similar to mouse taste organoids grown in suspension culture (70), our pig taste organoids grown in dynamic culture lacked apico-basal polarity. In dynamic culture, TRC-expressing cells can be found on the apical side and throughout the organoids (Fig. 3C), whereas in early passage static culture they are concentrated in the center surrounded by a stratified layer of proliferating cells (apico-basal) as shown in Fig. 1C.

Following on from our previous findings in rodent and human taste papillae (11), we successfully demonstrate that insulin is also transcribed and translated in pig taste papillae and papillae-derived taste organoids. We also addressed the question of the function(s) of lingual insulin. One intriguing possibility is that insulin is necessary for taste papillae/TRC development. It was already reported that increased concentration of insulin in culture media was detrimental to the expression of mature TRC and taste progenitor cell markers in rodent taste organoids (56). Our pig organoids, however, thrived in LPM supplemented with comparable high insulin concentrations. In fact, an insulin concentration of 10 nM or higher was essential for the normal growth and differentiation of pig taste organoids. The behavior was similar when insulin was replaced with either IGF1 or IGF2. When compared to each other, IGF2 upregulated the expression of taste progenitor cell and mature TRC markers significantly more than IGF1, particularly at concentrations 20 ng/mL and above. This could be attributed to the trophic action of IGF2 being mediated through the insulin receptor (78). Of interest, brain organoids also require insulin for their growth and differentiation (79), and insulin/IGFs have been described to play an essential role in the maintenance and neuronal development of the central nervous system (80). While insulin supplementation is required for organoid development, the potential contribution of endogenously produced insulin to organoid growth or progenitor maintenance has not been assessed. Given the expression of insulin in a subset of cells, it is possible that locally produced insulin may act in an autocrine or paracrine fashion to support epithelial renewal, independent of systemic glucose levels, which this model could be used to test.

We then examined the possibility of modifying C5 to increase insulin protein levels in our taste organoids. Inhibiting the expression of the transcription factor FOXO1 is known to promote the generation of insulin-producing cells in human induced pluripotent stem cells derived gut organoids (68); however, the addition of a small molecular inhibitor of FOXO1 did not increase insulin transcription in the organoids grown in C5. We then used quiescence-inducing factors as described in the literature (61) to further modify the C5 media and arrive at CQ media that induces >1000-fold increase in the expression of insulin and its transcription factors (*MAFA* and *PAX4*) in the taste organoids. The organoids were grown in LPM from days 0 to 10, subsequently transferred to C5/CQ media at the end of day 10, and harvested on day 16, giving them enough time to differentiate and produce mature TRCs. CQ media drastically increased (~3700-fold increase) the expression of insulin and its transcription factors and produced organoids that were morphologically different from both C5 and LPM organoids.

The existence of serotonin and its receptors leads us to hypothesize that insulin expression in this context is under serotonin control; this is in line with our previous work on the expression of insulin and regulation of insulin secretion in choroid plexus (12). Exogenous/endogenous serotonin is likely acting via the HTR1 family of serotonin receptors, whose expression was already previously reported in rat type II taste cells (69) and confirmed to be the serotonin receptor with the highest levels of expression in our pig taste organoids [Supplementary Fig. S6D (31)], leading to inactivation of adenylyl cyclase and consequent reduction of intracellular cAMP.

The choice of the pig to study taste organoids is not an esoteric one and is grounded in the knowledge that human physiology (81, 82) and somatic stem cell growth and differentiation (83) are more akin to that of pigs than rodents. Given their similarity to humans, kidneys from genetically modified pigs have now been safely transplanted into humans to successfully resolve renal failure (84, 85). As we have been able to culture the taste organoids long term, we have demonstrated the potential for unlimited expansion in vitro, negating the need to routinely house and euthanize pigs for this particular purpose. From a physiological standpoint and for the sake of completeness, it will be necessary to know exactly how lingual insulin transcription, translation, and release are regulated. As for potential functions above and beyond being required for taste stem cell growth and differentiation, whether lingual insulin acts a modifier of taste perception or plays a role in local muscle structure and function or local fat deposition in the posterior of the tongue remain to be studied.

A limitation of this study is that due to constraints in available experimental resources, we were unable to validate most findings at the protein level. We found very few antibodies that reliably cross-react with pig proteins, and the somatic cell markers LGR4/5/6 are very lowly expressed, such that organoid researchers normally rely on endogenous labels to detect protein expression of the cells both in mouse (6) and genome editing of the LGR5 locus with reporter labeling in human organoids (86). Furthermore, while some transcriptional parallels exist between TRC lineages and pancreatic β cells, these comparisons warrant further investigation, which could be facilitated by comparing transcriptomic and proteomic data from taste organoids directly with those from islets. Therefore, the work reported herein provides a platform for studying insulin expression in taste organoids and to understand extra-pancreatic insulin release and function.

Acknowledgments

This research was supported by the Intramural Research Program of the National Institutes of Health (NIH). The contributions of the NIH authors were made as part of their official duties as NIH federal employees, are in compliance with agency policy requirements, and are considered Works of the United States Government. However, the findings and conclusions presented in this paper are those of the authors and do not necessarily reflect the views of the NIH or the US Department of Health and Human Services.

We would like to thank Visual Media, specifically Lauren Brick, David Taylor, Marc Riley, and Aaron Russell for making the schemes shown throughout and for help with constructing and formatting the figures. This work utilized the computational resources of the NIH HPC Biowulf cluster (https://hpc.nih.gov).

Downloaded from https://academic.oup.com/endo/article/166/9/bqaf126/8221664 by Odense Universitetsbibliotek user on 21 April 2026

Author Contributions

Conceptualization, J.M.E. and M.E.D.; conducted experiments, H.U.P., C.H.M., M.E.D.; treated CHO cells and generated Western blots, J.F.O.C.; immunostaining, Q.Y.; hematoxylin and eosin staining, N.V.; performed bioinformatics analysis, H.U.P., M.E.D., C.W., G.L., S.D.; performed gene set enrichment analysis, J.C., H.U.P.; scRNA-Seq, D.T., G.L., J.F., S.D., and H.U.P.; writing—original draft, H.U.P., M.E.D.; visualization, H.U.P., M.E.D., G.L.; helped in designing/providing key insights and writing, C.H.M., P.S., D.T.; project administration, J.M.E.; writing—review & editing, H.U.P., M.E.D., J.M.E., P.S.; supervision, J.M.E. and M.E.D.

Disclosures

The authors have nothing to disclose

Data Availability

Original data generated and analyzed during this study are included in this published article or in the data repositories listed in References. The authors declare that the RNA sequencing data supporting the findings of this study have been deposited in NCBI's Gene Expression Omnibus (GEO) with GEO series accession number GSE252240 (22). Supplementary figures and tables are available at figshare: Supplementary Figures (30); Supplementary Video S1 (28); Supplementary Table S1 (15); Supplementary Table S2 (31); Supplementary Table S3 (43); Supplementary Table S4 (62).

References

1. Doyle ME, Appleton A, Liu QR, Yao Q, Mazucanti CH, Egan JM. Human type II taste cells express angiotensin-converting enzyme 2 and are infected by severe acute respiratory syndrome coronavirus 2 (SARS-CoV-2). *Am J Pathol*. 2021;191(9):1511-1519.
2. Doyle ME, Premathilake HU, Yao Q, Mazucanti CH, Egan JM. Physiology of the tongue with emphasis on taste transduction. *Physiol Rev*. 2023;103(2):1193-1246.
3. Yao Q, Doyle ME, Liu Q-R, *et al*. Long-term dysfunction of taste papillae in SARS-CoV-2. *NEJM Evid*. 2023;2(9).
4. Perea-Martinez I, Nagai T, Chaudhari N. Functional cell types in taste buds have distinct longevities. *PLoS One*. 2013;8(1):e53399.
5. Martens K, Steelant B, Bullens DMA. Taste receptors: the gatekeepers of the airway epithelium. *Cells*. 2021;10(11):2889.
6. Sato T, Vries RG, Snippert HJ, *et al*. Single Lgr5 stem cells build crypt-villus structures in vitro without a mesenchymal niche. *Nature*. 2009;459(7244):262-265.
7. Ren W, Lewandowski BC, Watson J, *et al*. Single Lgr5- or Lgr6-expressing taste stem/progenitor cells generate taste bud cells ex vivo. *Proc Natl Acad Sci U S A*. 2014;111(46):16401-16406.
8. Shechtman LA, Scott JK, Larson ED, *et al*. High Sox2 expression predicts taste lineage competency of lingual progenitors in vitro. *Development*. 2023;150(4):dev201375.
9. Shin YK, Martin B, Golden E, *et al*. Modulation of taste sensitivity by GLP-1 signaling. *J Neurochem*. 2008;106(1):455-463.
10. Elson AE, Dotson CD, Egan JM, Munger SD. Glucagon signaling modulates sweet taste responsiveness. *FASEB J*. 2010;24(10):3960-3969.
11. Doyle ME, Fiori JL, Gonzalez Mariscal I, *et al*. Insulin is transcribed and translated in mammalian taste bud cells. *Endocrinology*. 2018;159(9):3331-3339.
12. Mazucanti CH, Liu QR, Lang D, *et al*. Release of insulin produced by the choroid plexis is regulated by serotonergic signaling. *JCI Insight*. 2019;4(23):e131682.
13. Ribitsch I, Baptista PM, Lange-Consiglio A, *et al*. Large animal models in regenerative medicine and tissue engineering: to do or not to do. *Front Bioeng Biotechnol*. 2020;8:972.
14. Roura E, Koopmans SJ, Lallès JP, *et al*. Critical review evaluating the pig as a model for human nutritional physiology. *Nutr Res Rev*. 2016;29(1):60-90.
15. Premathilake HU, Mazucanti CH, Yao Q, *et al*. Supplemental table to: Pig Taste Cell-Derived Organoids Synthesize Insulin. figshare. Date of deposit 8 August 2025. https://figshare.com/s/0213155f7c00070a7e4f
16. Park D, Pandey SK, Maksimova E, Kole S, Bernier M. Akt-dependent antiapoptotic action of insulin is sensitive to farnesyltransferase inhibitor. *Biochemistry*. 2000;39(41):12513-12521.
17. Subramanian A, Tamayo P, Mootha VK, *et al*. Gene set enrichment analysis: a knowledge-based approach for interpreting genome-wide expression profiles. *Proc Natl Acad Sci U S A*. 2005;102(43):15545-15550.
18. Liberzon A, Birger C, Thorvaldsdóttir H, Ghandi M, Mesirov JP, Tamayo P. The molecular signatures database (MSigDB) hallmark gene set collection. *Cell Syst*. 2015;1(6):417-425.
19. Liberzon A, Subramanian A, Pinchback R, Thorvaldsdóttir H, Tamayo P, Mesirov JP. Molecular signatures database (MSigDB) 3.0. *Bioinformatics*. 2011;27(12):1739-1740.
20. Castanza AS, Recla JM, Eby D, Thorvaldsdóttir H, Bult CJ, Mesirov JP. Extending support for mouse data in the molecular signatures database (MSigDB). *Nat Methods*. 2023;20(11):1619-1620.
21. Das JK, Banskota N, Candia J, *et al*. Calorie restriction modulates the transcription of genes related to stress response and longevity in human muscle: the CALERIE study. *Aging Cell*. 2023;22(12):e13963.
22. Premathilake HU, Yao Q, Vegesna N, O'Connell JF, Egan JM, Doyle ME. Data from: Pig Taste Cell-Derived Organoids Synthesize Insulin. *NCBI Gene Expression Omnibus*. GEO Series accession GSE252240. Date of deposit 29 December 2023. https://www.ncbi.nlm.nih.gov/geo/query/acc.cgi?acc=GSE252240
23. Hao Y, Hao S, Andersen-Nissen E, *et al*. Integrated analysis of multimodal single-cell data. *Cell*. 2021;184(13):3573-3587.e29.
24. Hafemeister C, Satija R. Normalization and variance stabilization of single-cell RNA-seq data using regularized negative binomial regression. *Genome Biol*. 2019;20(1):296.
25. Kuleshov MV, Jones MR, Rouillard AD, *et al*. Enrichr: a comprehensive gene set enrichment analysis web server 2016 update. *Nucleic Acids Res*. 2016;44(W1):W90-W97.
26. Zhang C, Oakley B. The distribution and origin of keratin 20-containing taste buds in rat and human. *Differentiation*. 1996;61(2):121-127.
27. Miura H, Kusakabe Y, Hashido K, Hino A, Ooki M, Harada S. The glossopharyngeal nerve controls epithelial expression of Sprr2a and Krt13 around taste buds in the circumvallate papilla. *Neurosci Lett*. 2014;580:147-152.
28. Premathilake HU, Mazucanti CH, Yao Q, *et al*. Supplemental video to: Pig Taste Cell-Derived Organoids Synthesize Insulin. *figshare*. Date of deposit 8 August 2025. https://figshare.com/s/ec77a276d7b593ad15a2
29. Hewitt RJ, Lloyd CM. Regulation of immune responses by the airway epithelial cell landscape. *Nat Rev Immunol*. 2021;21(6):347-362.
30. Premathilake HU, Mazucanti CH, Yao Q, *et al*. Supplemental figures to: Pig Taste Cell-Derived Organoids Synthesize Insulin. *figshare*. Date of deposit 8 August 2025. https://figshare.com/s/d21c3047a432e81bcecc
31. Premathilake HU, Mazucanti CH, Yao Q, *et al*. Supplemental table to: Pig Taste Cell-Derived Organoids Synthesize Insulin. *figshare*. Date of deposit 8 August 2025. https://figshare.com/s/dd85b80112cd3d15505e
32. Barrett AW, Cort EM, Patel P, Berkovitz BK. An immunohistological study of cytokeratin 20 in human and mammalian oral epithelium. *Arch Oral Biol*. 2000;45(10):879-887.

Downloaded from https://academic.oup.com/endo/article/166/9/bqaf126/8221664 by Odense Universitetsbibliotek user on 21 April 2026

33. Witt M, Kasper M. Distribution of cytokeratin filaments and vimentin in developing human taste buds. *Anat Embryol (Berl)*. 1999;199(4):291-299.
34. Wang H, Iguchi N, Rong Q, *et al.* Expression of the voltage-gated potassium channel KCNQ1 in mammalian taste bud cells and the effect of its null-mutation on taste preferences. *J Comp Neurol*. 2009;512(3):384-398.
35. Vandenbeuch A, Anderson CB, Parnes J, *et al.* Role of the ectonucleotidase NTPDase2 in taste bud function. *Proc Natl Acad Sci U S A*. 2013;110(36):14789-14794.
36. Clapp TR, Trubey KR, Vandenbeuch A, *et al.* Tonic activity of Galpha-gustducin regulates taste cell responsivity. *FEBS Lett*. 2008;582(27):3783-3787.
37. Dutta Banik D, Martin LE, Freichel M, Torregrossa AM, Medler KF. TRPM4 and TRPM5 are both required for normal signaling in taste receptor cells. *Proc Natl Acad Sci U S A*. 2018;115(4):E772-eE781.
38. Liang Z, Wilson CE, Teng B, Kinnamon SC, Liman ER. The proton channel OTOP1 is a sensor for the taste of ammonium chloride. *Nat Commun*. 2023;14(1):6194.
39. Tanaka T, Komai Y, Tokuyama Y, *et al.* Identification of stem cells that maintain and regenerate lingual keratinized epithelial cells. *Nat Cell Biol*. 2013;15(5):511-518.
40. Ohmoto M, Lei W, Yamashita J, Hirota J, Jiang P, Matsumoto I. SOX2 regulates homeostasis of taste bud cells and lingual epithelial cells in posterior tongue. *PLoS One*. 2020;15(10):e0240848.
41. Okubo T, Clark C, Hogan BL. Cell lineage mapping of taste bud cells and keratinocytes in the mouse tongue and soft palate. *Stem Cells*. 2009;27(2):442-450.
42. Iwasaki S, Aoyagi H, Yoshizawa H. Localization of keratins 13 and 14 in the lingual mucosa of rats during the morphogenesis of circumvallate papillae. *Acta Histochem*. 2011;113(4):395-401.
43. Premathilake HU, Mazucanti CH, Yao Q, *et al.* Supplemental table to: Pig Taste Cell-Derived Organoids Synthesize Insulin. *figshare*. Date of deposit 8 August 2025. https://figshare.com/s/7ed6c68c408a0f634038
44. Ohmoto M, Nakamura S, Wang H, Jiang P, Hirota J, Matsumoto I. Maintenance and turnover of Sox2+ adult stem cells in the gustatory epithelium. *PLoS One*. 2022;17(9):e0267683.
45. Ren W, Aihara E, Lei W, *et al.* Transcriptome analyses of taste organoids reveal multiple pathways involved in taste cell generation. *Sci Rep*. 2017;7(1):4004.
46. Wauson Eric M, Zaganjor E, Lee AY, *et al.* The G protein-coupled taste receptor T1R1/T1R3 regulates mTORC1 and autophagy. *Mol Cell*. 2012;47(6):851-862.
47. Sukumaran SK, Palayyan SR. Sweet taste signaling: the core pathways and regulatory mechanisms. *Int J Mol Sci*. 2022;23(15):8225.
48. Shechtman LA, Piarowski CM, Scott JK, Golden EJ, Gaillard D, Barlow LA. Generation and culture of lingual organoids derived from adult mouse taste stem cells. *J Vis Exp*. 2021;(170). Doi: 10.3791/62300
49. Aihara E, Mahe MM, Schumacher MA, *et al.* Characterization of stem/progenitor cell cycle using murine circumvallate papilla taste bud organoid. *Sci Rep*. 2015;5(1):17185.
50. Pleguezuelos-Manzano C, Puschhof J, van den Brink S, Geurts V, Beumer J, Clevers H. Establishment and culture of human intestinal organoids derived from adult stem cells. *Curr Protoc Immunol*. 2020;130(1):e106.
51. Boonekamp KE, Kretzschmar K, Wiener DJ, *et al.* Long-term expansion and differentiation of adult murine epidermal stem cells in 3D organoid cultures. *Proc Natl Acad Sci U S A*. 2019;116(29):14630-14638.
52. Driehuis E, Kolders S, Spelier S, *et al.* Oral mucosal organoids as a potential platform for personalized cancer therapy. *Cancer Discov*. 2019;9(7):852-871.
53. Wrzesinski K, Frandsen HS, Calitz C, Gouws C, Korzeniowska B, Fey SJ. Clinostat 3D cell culture: protocols for the preparation and functional analysis of highly reproducible, large, uniform spheroids and organoids. *Methods Mol Biol*. 2021;2273:17-62.
54. Gaillard D, Xu M, Liu F, Millar SE, Barlow LA. β-Catenin signaling biases multipotent lingual epithelial progenitors to differentiate and acquire specific taste cell fates. *PLoS Genet*. 2015;11(5):e1005208.
55. Liotta AS, Kole HK, Fales HM, Roth J, Bernier M. A synthetic trissulfotyrosyl dodecapeptide analogue of the insulin receptor 1146-kinase domain inhibits tyrosine dephosphorylation of the insulin receptor in situ. *J Biol Chem*. 1994;269(37):22996-23001.
56. Takai S, Watanabe Y, Sanematsu K, *et al.* Effects of insulin signaling on mouse taste cell proliferation. *PLoS One*. 2019;14(11):e0225190.
57. Jones KB, Furukawa S, Marangoni P, *et al.* Quantitative clonal analysis and single-cell transcriptomics reveal division kinetics, hierarchy, and fate of oral epithelial progenitor cells. *Cell Stem Cell*. 2019;24(1):183-192.e8.
58. Wang J, Elghazi L, Parker SE, *et al.* The concerted activities of Pax4 and Nkx2.2 are essential to initiate pancreatic beta-cell differentiation. *Dev Biol*. 2004;266(1):178-189.
59. Cha J, Tong X, Coate KC, *et al.* Defining unique structural features in the MAFA and MAFB transcription factors that control insulin gene activity. *J Biol Chem*. 2024;300(12):107938.
60. Kitamoto T, Lee YK, Sultana N, *et al.* Chemical induction of gut β-like-cells by combined FoxO1/notch inhibition as a glucose-lowering treatment for diabetes. *Mol Metab*. 2022;66:101624.
61. Basak O, Beumer J, Wiebrands K, Seno H, van Oudenaarden A, Clevers H. Induced quiescence of lgr5+ stem cells in intestinal organoids enables differentiation of hormone-producing enteroendocrine cells. *Cell Stem Cell*. 2017;20(2):177-190.e4.
62. Premathilake HU, Mazucanti CH, Yao Q, *et al.* Supplemental table to: Pig Taste Cell-Derived Organoids Synthesize Insulin. *figshare*. Date of Deposit 8 August 2025. https://figshare.com/s/6facab1f04cc5b717a17
63. Dashti M, Nizam R, John SE, *et al.* ONECUT1 variants beyond type 1 and type 2 diabetes: exploring clinical diversity and epigenetic associations in Arab cohorts. *Front Genet*. 2023;14:1254833.
64. Artner I, Blanchi B, Raum JC, *et al.* Mafb is required for islet β cell maturation. *Proc Natl Acad Sci U S A*. 2007;104(10):3853-3858.
65. Russ-Silsby J, Patel KA, Laver TW, *et al.* The role of ONECUT1 variants in monogenic and type 2 diabetes Mellitus. *Diabetes*. 2023;72(11):1729-1734.
66. Yan W, Sunavala G, Rosenzweig S, Dasso M, Brand JG, Spielman AI. Bitter taste transduced by PLC-beta(2)-dependent rise in IP(3) and alpha-gustducin-dependent fall in cyclic nucleotides. *Am J Physiol Cell Physiol*. 2001;280(4):C742-C751.
67. Ubuka T. Subchapter 131D—Serotonin. In: Ando H, Ukena K, Nagata S, eds. *Handbook of Hormones*. 2nd ed. Academic Press; 2021:1049-1051.
68. Bouchi R, Foo KS, Hua H, *et al.* FOXO1 inhibition yields functional insulin-producing cells in human gut organoid cultures. *Nat Commun*. 2014;5(1):4242.
69. Jaber L, Zhao FL, Kolli T, Herness S. A physiologic role for serotonergic transmission in adult rat taste buds. *PLoS One*. 2014;9(11):e112152.
70. Adpaikar AA, Zhang S, Kim HY, *et al.* Fine-tuning of epithelial taste bud organoid to promote functional recapitulation of taste reactivity. *Cell Mol Life Sci*. 2022;79(4):211.
71. Merker SR, Weitz J, Stange DE. Gastrointestinal organoids: how they gut it out. *Dev Biol*. 2016;420(2):239-250.
72. Barlow LA, Klein OD. Developing and regenerating a sense of taste. *Curr Top Dev Biol*. 2015;111:401-419.
73. Prochazkova M, Häkkinen TJ, Prochazka J, *et al.* FGF signaling refines Wnt gradients to regulate the patterning of taste papillae. *Development*. 2017;144(12):2212-2221.
74. Yu W, Wang Z, Marshall B, *et al.* Taste buds are not derived from neural crest in mouse, chicken, and zebrafish. *Dev Biol*. 2021;471:76-88.
75. Fujii S, Suzuki K, Kawamoto A, *et al.* PGE2 is a direct and robust mediator of anion/fluid secretion by human intestinal epithelial cells. *Sci Rep*. 2016;6(1):36795.
76. Lee B-C, Kim H-S, Shin T-H, *et al.* PGE2 maintains self-renewal of human adult stem cells via EP2-mediated autocrine signaling and its

Downloaded from https://academic.oup.com/endo/article/166/9/bqaf126/8221664 by Odense Universitetsbibliotek user on 21 April 2026

production is regulated by cell-to-cell contact. *Sci Rep*. 2016;6(1):26298.
77. Fan YY, Davidson LA, Callaway ES, Goldsby JS, Chapkin RS. Differential effects of 2- and 3-series E-prostaglandins on in vitro expansion of Lgr5+ colonic stem cells. *Carcinogenesis*. 2014;35(3):606-612.
78. An W, Hall C, Li J, *et al*. Activation of the insulin receptor by insulin-like growth factor 2. *Nat Commun*. 2024;15(1):2609.
79. Hong YJ, Lee SB, Choi J, Yoon SH, Do JT. A simple method for generating cerebral organoids from human pluripotent stem cells. *Int J Stem Cells*. 2022;15(1):95-103.
80. Réthelyi JM, Vincze K, Schall D, Glennon J, Berkel S. The role of insulin/IGF1 signalling in neurodevelopmental and neuropsychiatric disorders—evidence from human neuronal cell models. *Neurosci Biobehav Rev*. 2023;153:105330.
81. Perleberg C, Kind A, Schnieke A. Genetically engineered pigs as models for human disease. *Dis Model Mech*. 2018;11(1):dmm030783.
82. Lunney JK, Van Goor A, Walker KE, Hailstock T, Franklin J, Dai C. Importance of the pig as a human biomedical model. *Sci Transl Med*. 2021;13(621):eabd5758.
83. Hill ABT, Murphy YM, Polkoff KM, *et al*. A gene edited pig fmodel for studying LGR5(+) stem cells: implications for future applications in tissue regeneration and biomedical research. *Front Genome Ed*. 2024;6:1401163.
84. Judd E, Kumar V, Porrett PM, *et al*. Physiologic homeostasis after pig-to-human kidney xenotransplantation. *Kidney Int*. 2024;105(5):971-979.
85. Anand RP, Layer JV, Heja D, *et al*. Design and testing of a humanized porcine donor for xenotransplantation. *Nature*. 2023;622(7982):393-401.
86. Forster R, Chiba K, Schaeffer L, *et al*. Human intestinal tissue with adult stem cell properties derived from pluripotent stem cells. *Stem Cell Reports*. 2014;2(6):838-852.

Downloaded from https://academic.oup.com/endo/article/166/9/bqaf126/8221664 by Odense Universitetsbibliotek user on 21 April 2026